Three-Dimensional Surround Sound Systems Based on Spherical Harmonics*

M. A. POLETTI, *AES Member*

Industrial Research Limited, Lower Hutt, New Zealand
(m.poletti@irl.cri.nz)

The theory of recording and reproduction of three-dimensional sound fields based on spherical harmonics is reviewed and extended. Free-field, sphere, and general recording arrays are reviewed, and the mode-matching and simple source approaches to sound reproduction in anechoic environments are discussed. Both methods avoid the need for both monopole and dipole loudspeakers—as required by the Kirchhoff–Helmholtz integral. An error analysis is presented and simulation examples are given. It is also shown that the theory can be extended to sound reproduction in reverberant environments.

0 INTRODUCTION

Surround sound systems offer the potential for immersive sound field reproduction without requiring information about listener orientation or head shape. The sound field is reconstructed over a finite region of space, and a listener positioned in this region may in principle experience the original sound field, including diffraction around the head.

The theory of two-dimensional (2D) sound systems has received much attention, and a common implementation is the Ambisonics system [1]–[16]. For regularly spaced circular arrays, well-known panning functions may be derived by assuming an incident plane wave and applying a mode-matching procedure to determine the required loudspeaker weights as a function of the angle of incidence [2], [3], [5]. These functions are optimum at low frequencies, but at high frequencies reproduction is inaccurate. Furthermore, for irregular arrays the theoretical panning functions can produce large amplitudes, which are likely to be sensitive to amplitude and phase mismatches [5]. For both regular and irregular arrays, subjectively optimized panning functions are often derived, which have reduced amplitudes and which reduce subjective anomalies and sensitivity to errors [15], [16].

The theory of three-dimensional (3D) sound field recording and reproduction is receiving increasing attention due to the potential it offers for more accurate reconstruction than can be achieved with 2D systems, including height information. There are several approaches to the problem. The Kirchhoff–Helmholtz integral shows that reproduction is possible inside a region if the pressure and normal velocity are known on the surface of the region [17]. This is the basis for the wave field synthesis (WFS) approach [18]–[26]. In practice simplifications are possible; for example, monopole sources are sufficient, and only those transducers in the direction of the sound source are required [9], [12], [13]. Wave field synthesis has also been applied to sound field synthesis in a half-space [19], [21] and is often applied to reproduction over large areas, and so is more general than the reproduction of localized sound fields considered here.

A second approach is the inverse method, in which an inverse matrix is derived for a given geometry of loudspeakers and receiver positions, which allows the creation of the required sound pressure at a set of discrete points [27]–[31]. This method also includes crosstalk cancellation systems as a specific case. The third approach is the 3D Ambisonics approach, which is based on a spherical harmonic decomposition of the sound field [7]–[15].

This paper reviews and extends the theory of 3D sound systems based on spherical harmonics. The spherical harmonic/Bessel and Kirchhoff–Helmholtz descriptions of sound fields are introduced, and their equivalence for spherically bounded regions of space is demonstrated. Three methods of sound field recording are briefly considered: free-space directional microphone arrays, pressure microphones mounted in a sphere, and free-space arrays with variable radii. Methods for sound reproduction in anechoic environments are then considered. The mode-matching approach is described, and then the simple source method introduced, which demonstrates formally

*Manuscript received 2005 March 18; revised 2005 September 27.

that sound fields may be recreated without requiring the use of dipole loudspeakers. The error performance of both methods is considered, means of controlling the error are described, and examples of sound field synthesis with each approach are given. Finally it is shown that the mode-matching approach can be extended to reproduction in reverberant environments with nonideal loudspeakers.

1 DESCRIPTION OF 3D SOUND FIELDS

A 3D sound field in the region of a point in space (taken to be the origin from here on) may be described in several ways. The Kirchhoff–Helmholtz integral is the mathematical form of Huyghen's principle. Alternatively, the sound field may be expanded in a Taylor series [32], [33] or a series of cylindrical or spherical coordinate eigenfunctions with corresponding cylindrical or spherical Bessel radial functions [17]. Dickens and Kennedy have shown that for solutions to the wave equation, the Taylor series expansion is equivalent to the spherical expansion, but less compact [32]. The cylindrical expansion—while a useful basis for a description of 2D systems [9], [12], [13], [23]—is less applicable to the 3D case as it involves infinite integrals over z [17]. We therefore consider only the spherical harmonic/Bessel and Kirchhoff–Helmholtz descriptions.

1.1 Spherical Harmonics/Spherical Bessel Description

In spherical coordinates (r, θ, ϕ) the solution to the wave equation may be written in terms of spherical Bessel functions and spherical harmonics [17]. For the interior case, where all sources lie outside the region of interest, the spatial variation of the sound field at a spatial frequency $k = \omega/c$, with c being the speed of sound, may be expressed as

$$p(r, \theta, \phi, k) = \sum_{n=0}^{\infty} \sum_{m=-n}^{n} A_n^m(k)\, j_n(kr)\, Y_n^m(\theta, \phi) \tag{1}$$

where $j_n(x)$ is the spherical Bessel function of the first kind [34], and the spherical harmonics are defined as [17], [35]

$$Y_n^m(\theta, \phi) = \sqrt{\frac{(2n+1)}{4\pi}\frac{(n-|m|)!}{(n+|m|)!}}\, P_n^{|m|}(\cos\theta)\, e^{im\phi} \tag{2}$$

where $P_n^m(\cdot)$ is the associated Legendre function [17], [35] and $i = \sqrt{-1}$. Each spherical harmonic is the scaled product of an elevation term $P_n^m(\cos\theta)$ and an azimuthal term $\exp(im\phi)$. The real and imaginary parts of Y_n^m produce functions with $\cos(m\phi)$ and $\sin(m\phi)$ azimuthal responses, which occur in 2D Ambisonics theory.

An important feature of this expansion is that for small kr, that is, for low frequencies or small distances from the origin, the summation in n may be truncated to a finite value N with little error, because only the low-order spherical Bessel functions have significant values for small kr. The pressure is then accurately represented by a total of $(N+1)^2$ terms.

For the exterior case, where all sources lie within a region of space, the solution to the wave equation outside that region can be written as

$$p(r, \theta, \phi, k) = \sum_{n=0}^{\infty} \sum_{m=-n}^{n} B_n^m(k)\, h_n(kr)\, Y_n^m(\theta, \phi) \tag{3}$$

where $h_n(kr)$ is the spherical Hankel function,

$$h_n(kr) = j_n(kr) + i y_n(kr) \tag{4}$$

and $y_n(x)$ is the spherical Bessel function of the second kind [34].

A formula that will be useful in what follows is the Wronskian relationship [17]

$$j_n(x)\, h_n'(x) - j_n'(x)\, h_n(x) = \frac{i}{x^2}. \tag{5}$$

Spherical harmonics form an orthonormal basis for any function defined on a sphere [17],

$$f(\theta, \phi) = \sum_{n=0}^{\infty} \sum_{m=-n}^{n} A_n^m\, Y_n^m(\theta, \phi). \tag{6}$$

The spherical harmonics are orthonormal,

$$\int_0^{2\pi} \int_0^{\pi} Y_n^m(\theta, \phi)\, Y_k^p(\theta, \phi)^* \sin(\theta)\, d\theta\, d\phi = \delta_{nk}\delta_{mp} \tag{7}$$

where δ_{nk} is 0 for $n \neq k$ and 1 for $n = k$. This allows the coefficients in Eq. (6) to be found as

$$A_n^m = \int_0^{2\pi} \int_0^{\pi} f(\theta, \phi)\, Y_n^m(\theta, \phi)^* \sin(\theta)\, d\theta\, d\phi \tag{8}$$

which is the projection of Eq. (6) onto the (n, m)th spherical harmonic.

1.2 Plane and Spherical Wave Expansions

Two specific expansions will be required in the theory that follows. The spherical harmonic expansion of a plane wave arriving from incidence angles (θ_i, ϕ_i) is [17]

$$e^{ik_i \cdot r} = 4\pi \sum_{n=0}^{\infty} i^n\, j_n(kr) \sum_{m=-n}^{n} Y_n^m(\theta, \phi)\, Y_n^m(\theta_i, \phi_i)^*. \tag{9}$$

The spherical harmonic expansion of the wavefield due to a point source with position (r_s, θ_s, ϕ_s), and with $r < r_s$, is [17], [35]

$$G(\boldsymbol{r}|\boldsymbol{r}_s) = \frac{e^{ik|\boldsymbol{r}-\boldsymbol{r}_s|}}{4\pi\,|\boldsymbol{r}-\boldsymbol{r}_s|} = ik \sum_{n=0}^{\infty} j_n(kr)\, h_n(kr_s) \sum_{m=-n}^{n} Y_n^m(\theta, \phi)\, Y_n^m(\theta_s, \phi_s)^*. \tag{10}$$

We will follow the convention in [17] of assuming a harmonic dependency $\exp(-i\omega t)$, so that the phase of Eq. (10) corresponds to waves propagating outward from $\boldsymbol{r}_s$ (since as t increases $|\boldsymbol{r} - \boldsymbol{r}_s|$ must increase to maintain the same phase).

1.3 Kirchhoff–Helmholtz Description

The Kirchhoff–Helmholtz integral shows that the sound pressure within an arbitrarily shaped volume of space may be calculated from the pressure and normal velocity on its surface [9], [12], [13], [17], [19]. For positions $\boldsymbol{r}$ within the surface S, the pressure is given by

$$p(\boldsymbol{r}) = \int_S \int \left[G(\boldsymbol{r}|\boldsymbol{r}_s) \frac{\delta p(r_s)}{\delta n} - p(r_s) \frac{\delta}{\delta n} [G(\boldsymbol{r}|\boldsymbol{r}_s)] \right] \mathrm{d}S \tag{11}$$

where n denotes the outward facing normal to the surface, and where $G(\boldsymbol{r}|\boldsymbol{r}_s)$ is the free-space Green's function defined in Eq. (10).

This shows that the sound field may be reproduced from an infinite distribution of monopole sources excited by the normal gradient of the pressure on the surface, and an infinite distribution of dipole sources excited by the pressure on the surface. In practice, since most loudspeakers are monopoles at low frequencies, the dipole sources are less practical to implement (requiring, for example, unbaffled drivers). It has been shown in [9], [12], [13], [20] that the monopole and dipole sources are not independent and that in practice the dipole sources may be ignored.

For the case of a spherical volume the Kirchhoff–Helmholtz integral can be shown to be equivalent to the spherical harmonic expansion of the sound field. The expansion for the Green's function is given in Eq. (10), and the pressure expansion is given in Eq. (1). For the spherical case the normal derivatives become radial, and the radial derivatives of the two expansions may be found easily. Substituting these four expansions into Eq. (11) and employing the orthonormality of the spherical harmonics yields

$$p(r, \theta, \phi, k) = -\mathrm{i}(kR)^2 \sum_{n=0}^{\infty} \sum_{m=-n}^{n} [j_n(kR)\, h_n'(kR) - j_n'(kR)\, h_n(kR)]\, j_n(kr)\, A_n^m(k)\, Y_n^m(\theta, \phi) \tag{12}$$

which, using the Wronskian expression [Eq. (5)] yields the expansion in Eq. (1). This shows that the Kirchhoff–Helmholtz integral is consistent with the spherical harmonic expansion of the sound field. Similarities between the Kirchhoff–Helmholtz and cylindrical expansions have also been considered in [9], [12], [13].

2 3D SOUND FIELD RECORDING

The accurate recording of sound fields requires the synthesis of higher directivities than are available from first-order microphones. These directivities can be obtained using microphone arrays. Array beamforming is a general approach that filters each microphone signal and sums the filter outputs to produce a desired polar response, and which can be applied to a variety of microphone array geometries [36]–[38]. Other methods have been proposed, such as the use of multiple discrete microphones [39], the combination of dipole responses [40], or single arrays with multiple radii [41]. Here we consider three methods for the direct computation of the spherical harmonic coefficients [41]–[46].

2.1 Free-Field Sphere Decomposition

Multiplying both sides of Eq. (1) by $Y_l^q(\theta, \phi)^*$ and integrating over the sphere [9], [43] yields

$$A_n^m(k) = \frac{1}{j_n(kr)} \int_0^{2\pi} \int_0^{\pi} p(r, \theta, \phi, k)\, Y_n^m(\theta, \phi)^* \sin(\theta)\, \mathrm{d}\theta\, \mathrm{d}\phi. \tag{13}$$

As in the 2D case [6], the zeros of $j_n(kr)$ produce equalization problems. One approach to removing the problem is to use first-order microphones facing radially outward [6], [9]. The general form of a radial first-order response is

$$s_\alpha(r, \theta, \phi, k) = \alpha p(r, \theta, \phi, k) - (1 - \alpha)\, \rho c v_R(r, \theta, \phi, k) \tag{14}$$

where α is the first-order parameter, v_R is the radial velocity, and ρc is the impedance of free space. The spherical harmonic expansion of the radial velocity may be obtained from Euler's equation [17] and Eq. (1). The first-order response then has the spherical harmonic expansion

$$s_\alpha(r, \theta, \phi, k) = \sum_{n=0}^{\infty} [\alpha j_n(kr) - \mathrm{i}(1 - \alpha)\, j_n'(kr)] \sum_{m=-n}^{n} A_n^m(k)\, Y_n^m(\theta, \phi) \tag{15}$$

and the spherical harmonic coefficients are [9]

$$A_n^m(k) = \frac{1}{\alpha j_n(kr) - \mathrm{i}(1 - a)\, j_n'(kr)} \times \int_0^{2\pi} \int_0^{\pi} s_\alpha(r, \theta, \phi, k)\, Y_n^m(\theta, \phi)^* \sin(\theta)\, \mathrm{d}\theta\, \mathrm{d}\phi. \tag{16}$$

The zeros of $j_n(kr)$ no longer produce infinite equalization responses. The responses produce minimum variations in magnitude with frequency for $\alpha = 0.5$, as in the 2D case. The ideal $\alpha = 0.5$ array response functions are shown in Fig. 1 for $n = 0, \ldots, 3$. They have a form similar to those in [6] for the 2D case.

2.2 Solid Sphere Decomposition

An alternative method for finding the coefficients has been introduced by Meyer and coworkers [44]–[46]. A solid sphere containing flush mounted pressure microphones also allows the coefficients to be found without the risk of zeros in the response.

The scattering of sound around a sphere for a sound field given in Eq. (1) is obtained by assuming that the resultant field is the sum of the original field and a scattered field that is radiating outward. The scattered field is

therefore expressed as in Eq. (3). The coefficients B_n^m are found by assuming that the sphere is solid and that the total radial velocity equals zero at the surface, yielding a total field [17]

$$p_t(r, \theta, \phi, k) = \sum_{n=0}^{\infty} \left[j_n(kr) - \frac{j_n'(ka)}{h_n'(ka)} h_n(kr) \right] \sum_{m=-n}^{n} A_n^m(k)\, Y_n^m(\theta, \phi) \tag{17}$$

where a is the radius of the sphere. This is the sum of the original wavefield without the sphere [Eq. (1)] and a scattering field consisting of outgoing waves whose coefficients are modified by a ratio of spherical Bessel terms. The sound field coefficients may be found from the pressure at $r = a$,

$$A_n^m(k) = \frac{1}{j_n(ka) - [j_n'(ka)/h_n'(ka)]\, h_n(ka)} \times \int_0^{2\pi} \int_0^{\pi} p_t(a, \theta, \phi, k)\, Y_n^m(\theta, \phi)^* \sin(\theta)\, d\theta\, d\phi. \tag{18}$$

The denominator in the fraction can, however, be simplified using the Wronskian expression as follows:

$$j_n(ka) - \frac{j_n'(ka)}{h_n'(ka)} h_n(ka) = \frac{1}{h_n'(ka)} [j_n(ka)\, h_n'(ka) - j_n'(ka)\, h_n(ka)] = \frac{i}{(ka)^2} \frac{1}{h_n'(ka)} \tag{19}$$

which yields

$$A_n^m(k) = -i(ka)^2\, h_n'(ka) \times \int_0^{2\pi} \int_0^{\pi} p_t(a, \theta, \phi, k)\, Y_n^m(\theta, \phi)^* \sin(\theta)\, d\theta\, d\phi. \tag{20}$$

The required equalization responses are shown in Fig. 2. They are smoother than the free-field responses in Fig. 1 at high frequencies. However, at low frequencies the free-space responses for $n > 0$ increase with frequency with order $(n - 1)$, whereas the sphere responses rise with order n. (These can be derived using the small argument limits for the Bessel functions [17].) The free-space response therefore requires less extreme low-frequency equalization (that is, a greater low-frequency range for a finite maximum equalization gain), but requires the use of cardioid microphones. In addition, diffraction around the microphones will produce more complicated frequency responses than those shown in Fig. 1. The sphere responses can use pressure microphones flush mounted in a sphere, which will produce responses closer to the theoretical responses than the free-field array.

2.3 General Sampling Array

A more general approach to the preceding is to use a sampling of the sound pressure field at M arbitrary positions. The field can be recreated at the same relative positions in a room using M loudspeakers if the matrix of transfer functions from the loudspeakers to those positions is known [28]. Alternatively the method can be applied to the measurement of spherical harmonics [41]. Expressing

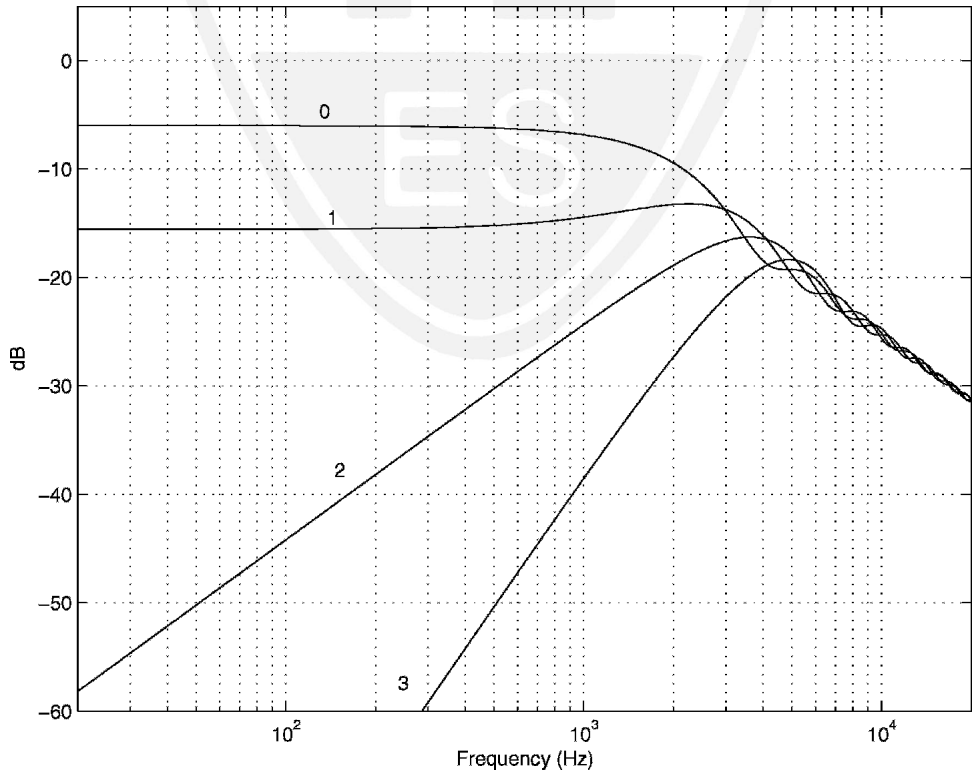

Fig. 1. Ideal free-field array responses for orders 0 to 3, $\alpha = 0.5$, assuming a sufficient number of microphones to ensure that alias effects lie above 20 kHz.

the pressure at M positions $p(r_m, \theta_m, \phi_m)$ as in Eq. (1), the vector of pressures p can be written

$$p = \Lambda A \tag{21}$$

where A is the vector of $K = (N + 1)^2$ spherical harmonic coefficients to be determined and Λ is the matrix with elements $j_n(kr_l)\, Y_n^m(\theta_l, \phi_l)$. Typically $M > K$, the system is overdetermined, and the vector of coefficients can then be obtained as the regularized least-squares inverse of Eq. (21) [41],

$$A = [\Lambda^\dagger \Lambda + \lambda I]^{-1}\, \Lambda^\dagger p \tag{22}$$

where λ is a regularization parameter, I is the $K \times K$ identity matrix, and † denotes the conjugate transpose. When the sample points are at the same radius r_0, then Eq. (21) can be written

$$p = Y J A \tag{23}$$

where Y is the matrix of spherical harmonic terms and J a diagonal matrix with elements $j_n(kr_0)$. If the positions are those of a regular polyhedron and $M = K$, then Λ is a unitary matrix and

$$A = J^{-1} Y^\dagger p \tag{24}$$

which is the discrete matrix form of Eq. (13). Hence the general approach includes the open-sphere approach as a special case. However, the use of multiple radii eliminates the zeros that occur in the free-field spherical array responses. It can also accommodate directional element responses [41]. The design challenge for such arrays is determining the geometry to produce a reasonable array response for all spherical harmonics over the required frequency range.

2.4 Sampling Requirements for Recording

Sound field recording using the ideal integrals in Eq. (16) or (20) produces the exact spherical harmonic coefficients. In practice recording is carried out using a finite number of discrete microphones in some 3D array. The sampling produces a response that is a sum of the desired spherical harmonic and a number of higher order alias harmonics, in a fashion similar to the 2D case [6], [9]. The determination of the alias components is more difficult in the 3D case because there is not a simple periodic interpretation to the spherical harmonics as occurs in the 2D case.

An important parameter for recording is the number of spatial samples required to accurately record over a given volume of space and bandwidth. For an arbitrary function of 3D space, the sampling theorem suggests that the entire volume must be sampled at at least two samples per wavelength for the highest wavelength present. However, an acoustic sound field is not an arbitrary function of space, since it is constrained by the wave equation. The Kirchhoff–Helmholtz integral shows that the sound field within a volume of space is completely determined by its pressure and radial velocity on the surface of the volume. It will be shown in Section 3.3 that the pressure alone is sufficient. We therefore consider a volume of space enclosed by a sphere of radius R, with a maximum frequency f_{max} and a wavelength λ_{min}. If we sample the pressure on the surface

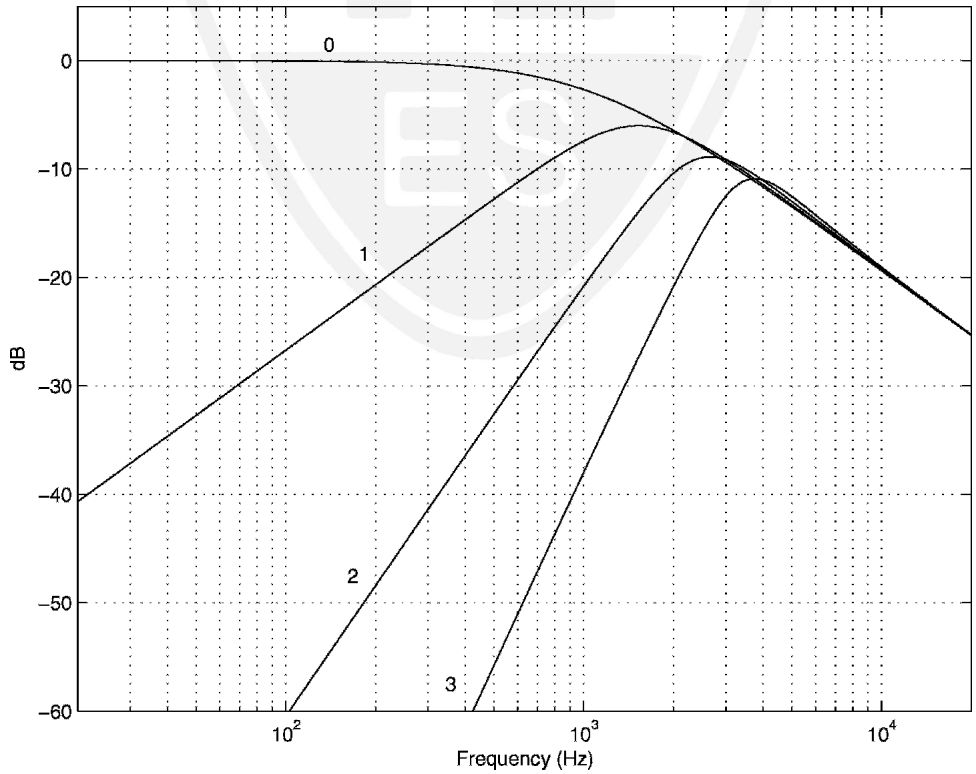

Fig. 2. Ideal sphere array responses for orders 0 to 3, assuming a sufficient number of microphones to ensure that alias effects lie above 20 kHz.

of the sphere at the Nyquist rate $\lambda_{min}/2$, the number of samples required is of the order

$$N_{samples} = 16\pi \left(\frac{R}{c} f_{max}\right)^2 = 50.2 \left(\frac{R}{c} f_{max}\right)^2 \quad (25)$$

which for a radius of 0.1 m requires 69 samples at $f_{max} = 4$ kHz and 278 samples at $f_{max} = 8$ kHz.

A more detailed approach is obtained using the spherical harmonic expansion in Eq. (1). From the previous section, with $(N + 1)^2$ samples, the spherical harmonic coefficients up to order N may be found. This approximates the sound field, and the error is the truncation error consisting of all terms in Eq. (1) higher than order N. By determining bounds on the envelope of $j_n(kr)$ the order N required to accurately represent the field can be determined. This approach is followed in [47], [48] and produces a 3D "dimensionality" of

$$N_{samples} = \left(\frac{e\pi R}{\lambda_{min}} + 1\right)^2 \approx 75 \left(\frac{R}{c} f_{max}\right)^2 \quad (26)$$

where $e = 2.718$, which is slightly larger than Eq. (25). We also note that this is approximately

$$N_{samples} \approx (k_{max} R + 1)^2 \approx 39.5 \left(\frac{R}{c} f_{max}\right)^2 \quad (27)$$

where k_{max} is the maximum wavenumber in the sound field.

3 3D SOUND FIELD REPRODUCTION

Several papers have considered the problem of recreating sound fields in anechoic environments using an array of loudspeakers [2]–[15], [49], [50]. In [2]–[6], [49] the creation of 2D plane wavefields is considered. In [50] the creation of 3D plane wavefields is considered, and in [9]–[14] the general 3D case is considered.

Many of these papers consider the synthesis of a sound field by matching the spherical harmonic amplitudes of the desired field with the sum of the spherical harmonic amplitudes produced by an ideal set of loudspeakers. In [50] the creation of 3D plane waves using spherical sources is considered and the loudspeaker weights are obtained using least-squares methods. A similar approach is given in [9]. This approach will be reviewed here, and then an alternative will be described based on the simple source approach [17]. The reconstruction error will be considered and examples given.

A limitation of the theory considered is that it does not take into account the reverberant nature of rooms, which tends to interfere with the direct sound field generated by the loudspeakers. In [51] a method is presented for 2D reproduction in reverberant rooms. It will be shown here that the spherical harmonic approach can also be extended to 3D reproduction in reverberant rooms and with nonideal loudspeakers.

3.1 Sampling Requirements for Reproduction

A rule of thumb is given in [50] for the number of loudspeakers L required to produce an accurate reconstruction of a plane wave for a given radius and frequency,

$$L \geq (\lceil kr \rceil + 1)^2 \quad (28)$$

where $\lceil . \rceil$ denotes rounding up to the nearest integer. This has a similar form as the equations for the number of samples for recording a sound field [Eqs (26) and (27)]. Hence, as might be expected, the sampling requirements for recording and reproducing a sound field up to a given order N are the same.

The radius of the head is about 87 mm [52], and the number of loudspeakers required at this radius for frequencies 1–16 kHz is shown in Table 1. The results for a larger radius of 100 mm, which more easily allows some head movement, are also given. The table shows that an accurate construction of 3D fields is not practical across the entire audio range. However, relatively large arrays of around 100 loudspeakers would allow reconstruction for a single listener up to 4 kHz, which would allow the majority of the sound field energy to be reproduced accurately and many of the directional cues to be recreated.

3.2 Mode-Matching Approach

We consider first the 3D equivalent of the Ambisonics plane wave matching equation. We synthesise a plane wave from arbitrary direction (θ_s, ϕ_s) using L plane wave sources with amplitudes w_l. This scenario is approximated if the L loudspeakers in a surround sound system are at a large distance from the listener. From Eq. (9) the synthesized field is

$$\hat{p}(r, \theta, \phi, k) = 4\pi \sum_{n=0}^{\infty} i^n j_n(kr) \sum_{m=-n}^{n} Y_n^m(\theta, \phi) \times \sum_{l=1}^{L} w_l(\theta_s, \phi_s)\, Y_n^m(\theta_l, \phi_l)^* \quad (29)$$

This must equal the plane wave expansion of the desired plane wave arriving from direction (θ_s, ϕ_s). The resulting matching equation for each n and m is

$$\sum_{l=1}^{L} w_l(\theta_s, \phi_s)\, Y_n^m(\theta_l, \phi_l)^* = Y_n^m(\theta_s, \phi_s)^* \quad (30)$$

This equation must be solved for the L weights $w_l(\theta_s, \phi_s)$ for all spherical harmonics up to some order N. Since the total number of spherical harmonics up to order N is $(N + 1)^2$, this requires $(N + 1)^2 \geq L$. The resulting $w_l(\theta_s, \phi_s)$ then specify a set of low-frequency panning functions for the lth loudspeaker. If the loudspeaker array is a 2D ring, then only the sectoral harmonics $m = n$ are required. This equation then reduces to the Ambisonics azimuthal mode-matching equation [3], [6].

Table 1. Required number of loudspeakers for reproduction over spheres of different radii R.

Frequency (Hz)	$R = 87$ mm	$R = 100$ mm
1000	9	9
2000	25	25
4000	64	81
8000	196	256
16 000	729	961

A more general approach is to assume that the L loudspeakers generate spherical waves. To synthesize a plane wave we equate the sum of L spherical waves [Eq. (10)] to a plane wave from direction (θ_s, ϕ_s), yielding

$$\sum_{l=1}^{L} w_l(\theta_s, \phi_s)\, Y_n^m(\theta_l, \phi_l)^* = \frac{\mathrm{i}^n}{\mathrm{i}kh_n(kR)}\, Y_n^m(\theta_s, \phi_s)^*. \tag{31}$$

This is equivalent to that in [50] apart from the phase of the Green's function [Eq. (10)] and a scale factor $\exp(-\mathrm{i}kr)/r$. The weights are again obtained by solving the set of equations for spherical harmonics up to order N.

If the source to be synthesized using spherical source loudspeakers is a single spherical source, then the matching equations become

$$\sum_{l=1}^{L} w_l(r_s, \theta_s, \phi_s)\, Y_n^m(\theta_l, \phi_l)^* = \frac{h_n(kr_s)}{h_n(kR)}\, Y_n^m(\theta_s, \phi_s)^* \tag{32}$$

which has been derived by Daniel and coworkers from the perspective of compensating for near-field loudspeakers and coding for source distance [9], [10]. The loudspeaker weights obtained from this set of equations are now panning functions which vary with the source radius. When the spherical source has the same radius as the loudspeakers ($r_s = R$), the panning functions reduce to the plane wave functions in Eq. (30). This means that the panning functions derived for idealized plane wave sources will also be optimum for the creation of spherical sources at the radius of the loudspeaker array.

For the general free-field case, the field due to spherical source loudspeakers is equated to the general solution of the wave equation in Eq. (1), yielding

$$\sum_{l=1}^{L} w_l Y_n^m(\theta_l, \phi_l)^* = \frac{A_n^m(k)}{\mathrm{i}kh_n(kR)}. \tag{33}$$

The weights w_l can no longer be interpreted as panning functions since they provide reproduction of multiple sources.

Eq. (33) may be written in matrix notation for all spherical harmonics up to order N as [9]

$$\Psi w = d \tag{34}$$

where the elements of the $(N+1)^2 \times L$ "mode" matrix Ψ are

$$\Psi_{v,l} = Y_n^m(\theta_l, \phi_l)^* \tag{35}$$

for $v = n^2 + n + m + 1$ for all values of n and m up to the maximum order N, and where d is the vector with elements

$$d_v = \frac{A_n^m(k)}{\mathrm{i}kh_n(kR)}. \tag{36}$$

d can be written $d = H^{-1} A$, where H is the diagonal matrix,

$$H = \begin{bmatrix} \mathrm{i}kh_0(kR) & 0 & 0 & 0 & \dots & 0 \\ 0 & \mathrm{i}kh_1(kR) & & & & \\ 0 & & \mathrm{i}kh_1(kR) & & & \\ 0 & & & \mathrm{i}kh_1(kR) & & \\ \dots & & & & \dots & \\ 0 & & & & & \mathrm{i}kh_N(kR) \end{bmatrix} \tag{37}$$

and A is the vector of spherical harmonic coefficients. Note that the nth Hankel function appears in H $2n + 1$ times.

If the number of modes to be matched is less than the number of loudspeakers, $(N+1)^2 < L$, then the system of mode-matching equations is under-determined and there are an infinite number of solutions. The weights with the minimum energy are obtained by minimizing the weight energy with the constraint Eq. (34), which yields [9], [50]

$$\hat{w} = \Psi^\dagger [\Psi\Psi^\dagger]^{-1} H^{-1} A. \tag{38}$$

If $(N+1)^2 = L$, then the weights can be found from the inverse

$$\hat{w} = \Psi^{-1} H^{-1} A. \tag{39}$$

Finally, if the number of modes exceeds the number of loudspeakers, $(N+1)^2 > L$, then there is no exact solution. Typically, the solution with the minimum least-squared error is derived. However, this solution can produce large weight magnitudes. The weight energy can be controlled by regularization, where a penalty function is added to the minimization. Using the energy in the weights $w^\dagger w$ as the penalty function controls the total power fed to the loudspeakers. The regularized solution is then obtained by minimizing

$$\hat{w} = \min_w \{\|\Psi w - d\|^2 + \lambda w^\dagger w\} \tag{40}$$

where λ is the regularization control parameter. The solution is

$$\hat{w} = [\Psi^\dagger\Psi + \lambda I]^{-1} \Psi^\dagger H^{-1} A \tag{41}$$

where I is the $L \times L$ identity matrix. The robustness of the solution depends on the eigenvalues of $\Psi\Psi^\dagger$, which are the squared singular values of Ψ. The regularization parameter may therefore be usefully specified as a scalar b times the minimum singular value in Ψ.

In practice it was found that the lowest error solutions were produced when $(N+1)^2 = L$. In this case all three solutions mentioned [with $\lambda = 0$ in Eq. (41)] are identical. However, the inverse is sensitive to the existence of small eigenvalues of Ψ. The regularized solution in Eq. (41) allowed the error to be controlled in a useful way, and was therefore used in the examples that follow.

3.3 Simple Source Approach

An alternative to the mode-matching approach will now be derived which does not require the calculation of inverse matrices.

It is shown in [17] that the Kirchhoff–Helmholtz integral is not the only way of recreating the sound field, and that either the pressure or the velocity on the surface is required, but not both. (This is also shown in the context of wave field synthesis in [9], [12], [13].) Williams shows that there are two approaches to simplying Eq. (11). One method is to employ a different Green's function from the free-space function used in Eq. (10), that is, one whose value on the surface S is zero (Dirichlet Green's function) or one whose normal derivative is zero (Neumann Green's function). This eliminates one of the two terms in Eq. (11). However, this approach requires sound sources that are impractical to produce.

The other method is to assume a simple monopole distribution and derive the excitation signals required to recreate the sound field, that is, it is assumed that the sound field can be reconstructed as

$$p(r, \theta, \phi, k) = \int\int_S \mu(\boldsymbol{r}_s) \frac{e^{ik|\boldsymbol{r}-\boldsymbol{r}_s|}}{4\pi\,|\boldsymbol{r}-\boldsymbol{r}_s|}\,dS. \tag{42}$$

The required distribution $\mu(\boldsymbol{r}_s)$ is obtained from the equivalent interior and exterior problems and by requiring that they produce the same pressure on the surface S [17]. Here we develop the simple source solution for the case of a spherical source distribution in an intuitive manner, and leave the proof to Appendix 1.

The spherical harmonic expansion of a monopole source is given in Eq. (10). Assume a reproduction system consisting of a continuous spherical distribution of monopole sources at radius R. Suppose that the monopole source amplitude at the position (θ_s, ϕ_s) is given by the spherical harmonic amplitude at that position $Y_n^m(\theta_s, \phi_s)$. The resulting field is the integration of all sources over the sphere. Substituting the expansion of the Green's function from Eq. (10) and using the orthogonality of the spherical harmonics, the resulting field is

$$\int_0^{2\pi}\int_0^{\pi} \frac{e^{ik|\boldsymbol{r}-\boldsymbol{r}_s|}}{4\pi\,|\boldsymbol{r}-\boldsymbol{r}_s|} Y_n^m(\theta_s, \phi_s)\, R^2 \sin(\theta_s)\, d\theta_s\, d\phi_s = ikR^2\, j_n(kr)\, h_n(kR)\, Y_n^m(\theta, \phi). \tag{43}$$

This contains the functions in one term of the expansion of the sound field [Eq. (1)] modified by a scaled Hankel function. Hence scaling the spherical harmonic amplitude by $A_n^m(k)$ and dividing by $ikR^2 h_n(kR)$ produces one term in the expansion of the sound field [Eq. (1)],

$$\int_0^{2\pi}\int_0^{\pi} \frac{e^{ik|\boldsymbol{r}-\boldsymbol{r}_s|}}{4\pi\,|\boldsymbol{r}-\boldsymbol{r}_s|} \frac{A_n^m(k)\, Y_n^m(\theta_s, \phi_s)}{ikR^2 h_n\,(kR)} R^2 \sin(\theta_s)\, d\theta_s\, d\phi_s = A_n^m(k)\, j_n(kr)\, Y_n^m(\theta, \phi). \tag{44}$$

This suggests that the sound field may be reconstructed as

$$p(r, \theta, \phi, k) = \int_0^{2\pi}\int_0^{\pi} \frac{e^{ik|\boldsymbol{r}-\boldsymbol{r}_s|}}{4\pi\,|\boldsymbol{r}-\boldsymbol{r}_s|} \left[\sum_{n=0}^{\infty}\sum_{m=-n}^{n} \frac{A_n^m(k)}{ikR^2 h_n(kR)} Y_n^m(\theta_s, \phi_s)\right] \times R^2 \sin(\theta_s)\, d\theta_s\, d\phi_s. \tag{45}$$

The term in brackets is the required monopole source amplitude at the angles (θ_s, ϕ_s). Appendix 1 shows that this is the simple source solution.

In practice the integral is replaced by a summation over L loudspeakers, and the lth weighting is given by the truncated series

$$w_l = \frac{g_l}{ik} \sum_{n=0}^{N}\sum_{m=-n}^{n} \frac{A_n^m(k)}{h_n(kR)} Y_n^m(\theta_l, \phi_l) \tag{46}$$

where g_l is a weighting term that arises from the finite sum approximation to the integral. This equation describes the encoding matrix for taking measured sound field coefficients $A_n^m(k)$ and producing the loudspeaker signals for a given loudspeaker geometry. Sets of angles and weighting functions (for radius 1) and various L are given at [53].

Eq. (46) can be written in matrix notation,

$$w = G\Psi^{\dagger}H^{-1}A \tag{47}$$

where G is the diagonal matrix of weights g_l. This is similar to the mode-match solution in Eqs. (39) and (41). In particular if $L = (N+1)^2$, $G = I$, and the mode matrix is unitary, $\Psi^{\dagger} = \Psi^{-1}$, then the mode-match solution Eq. (39) and simple source solutions are identical.

Daniel has shown that the transpose may be used when the loudspeaker geometry is regular [9], [11]. This occurs in equiangle 2D layouts. For the 3D case regular layouts based on polyhedra produce equal weights g_l, but Ψ is only approximately unitary, and so the mode-matching solution cannot be simplified. The simple source formulation shows that even when the mode matrix is not unitary, the solution in Eq. (47) is valid, but not in the least-squares mode-matching sense.

The performance of the simple source solution may be controlled by applying a window function $\Omega_n^m(k)$ to the spherical harmonics. This is the 3D equivalent of the windowing of the 2D Ambisonics signals [6], [9], [11], [15]. The weights are in this case given by

$$w_l = \frac{g_l}{ik} \sum_{n=0}^{N}\sum_{m=-n}^{n} \frac{A_n^m(k)}{h_n(kR)} \Omega_n^m\, Y_n^m(\theta_l, \phi_l) \tag{48}$$

which can be written in matrix form,

$$w = G\Psi^{\dagger}\Omega H^{-1}A \tag{49}$$

where Ω is the diagonal matrix of window elements. A simple form of window is

$$\Omega_n^m = W_1(n)\, W_2(m), \qquad n = 0{:}N, \quad m = -N{:}N \tag{50}$$

where W_1 is a one-sided window and W_2 is a length $2N+1$ symmetrical window. In the examples that follow an exponential window in n with control parameter δ $W_1(n) = \exp(-\delta n/N)$, and a Kaiser window in m will be used. An important requirement of any 2D window function is that it be equal to one for small n and m. This ensures that the simple source solution remains exact at the center of the loudspeaker array.

3.4 Error Performance

The performance of the mode-matching and simple source approaches can be quantified analytically assuming ideal spherical loudspeaker sources and an anechoic environment by determining the normalized radial error [50]

$$\bar{\varepsilon}(r,k)=\frac{\int_0^{2\pi}\int_0^{\pi}|p(r,\theta,\phi,k)-\hat{p}(r,\theta,\phi,k)|^2\sin(\theta)\,d\theta\,d\phi}{\int_0^{2\pi}\int_0^{\pi}|p(r,\theta,\phi,k)|^2\sin(\theta)\,d\theta\,d\phi} \tag{51}$$

where $\hat{p}(r, \theta, \phi, k)$ is the field approximated by the reproduction system. This form can be calculated relatively easily using spherical harmonic expansion formulas (Appendix 2).

There are two normalized radial errors of interest. The first is the theoretical truncation error caused by the truncation of the spherical source expansion in Eq. (10) to a maximum $n = N$. This ignores the aliasing caused by having a finite number of loudspeakers. The truncation error therefore represents a lower bound on the reproduced error. For a spherical source the normalized truncation error is

$$\bar{\varepsilon}_T(r,k)=1-\frac{\sum_{n=0}^{N}(2n+1)\,j_n^2(kr)\,|h_n(kr_s)|^2}{\sum_{n=0}^{\infty}(2n+1)\,j_n^2(kr)\,|h_n(kr_s)|^2}. \tag{52}$$

This is the spherical source equivalent of the plane wave truncation error in [50].

The truncation errors are shown in Fig. 3 for a source radius of 2.5 m for maximum orders up to 18 (requiring a minimum of 361 loudspeakers). The truncation errors for larger source radii are very similar, and the spherical errors are also very similar to those for the plane wave case given in [50]. The rule-of-thumb value of 4% (−14 dB) for an order equal to kr given in [50] is confirmed for spherical sources.

The second error of interest is the actual reproduced field error for a given source position (R_s, θ_s, ϕ_s) and set of loudspeaker weights. This error includes both the truncation error and the aliasing error caused by the finite number of loudspeakers used. It is given by

$$\bar{\varepsilon}_F(r,k)=4\pi\left[\sum_{n=0}^{\infty}\sum_{m=-n}^{n}j_n^2(kr)\,|h_n(kR)\sum_{l=0}^{\infty}w_l Y_n^m(\theta_l,\phi_l)^* - h_n(kr_s)\,Y_n^m(\theta_s,\phi_s)^*|^2\right] \times\left[\sum_{n=0}^{\infty}(2n+1)\,j_n^2(kr)|h_n(kr_s)|^2\right]^{-1}. \tag{53}$$

Fig. 4 shows the mode-matching and simple source field errors for a 100-loudspeaker layout with a loudspeaker radius of 2 m and a source position of 2.5 m, azimuth 0°, and elevation 90°. The maximum spherical harmonic order used is 9. The truncation error is also shown for reference.

Without regularization, the mode-matching error tends to zero for small kr. This occurs because the expansion in Eq. (1) requires only a small number of terms for small kr. The mode-matching solution thus becomes exact when the required order in Eq. (1) reduces below the order of the mode-matching equations. As kr increases, the required

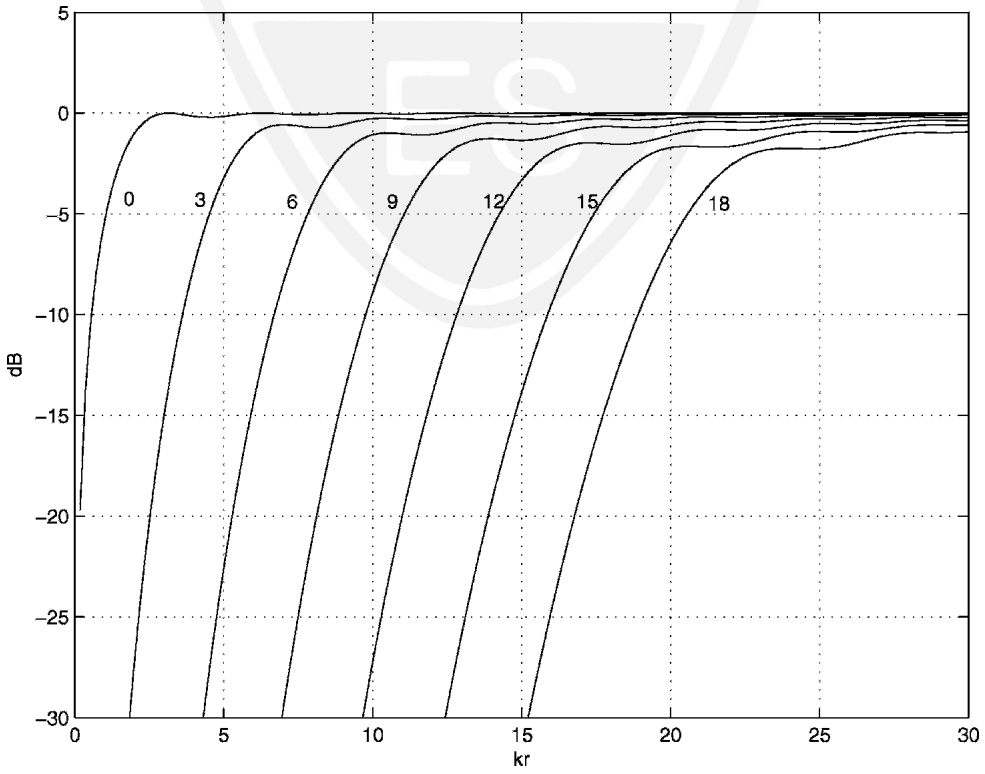

Fig. 3. Average truncation error for spherical source at 2.5-m radius.

order exceeds the order of the mode-matching equations, and the mode-matching field error increases rapidly. With a regularization parameter of $b = 2$ the mode-matching error increases to a constant value at small *kr,* but the error is not as large at large *kr* as for the unregularized solution.

The unwindowed simple source field error is greater than the unregularized mode-matching error at small *kr* because it does not attempt to minimize the error as the mode-matching solution does. However, the simple source error is lower than the unregularized mode-matching error at large *kr*. Regularization reduces the mode-matching error to slightly below the simple source error at large *kr*. However, with windowing the simple source error at large *kr* is lower than the regularized mode-matching solution. The mode-matching error could be further reduced by using a higher regularization value with a further reduction in accuracy at small *kr*. It is clear that a variety of trade-off solutions are possible for either method. However, the simple source solution appears to offer an effective alternative to the least-squares approach, and has the advantage that the error remains small at low *kr*.

3.5 Examples

We now consider some specific examples to demonstrate the performance of the mode-matching and simple source methods in an anechoic environment. We use a 100-loudspeaker spherical array of monopoles at a radius of 2 m. The maximum spherical harmonic order with this number is $N = 9$. To simplify the visualization of the 3D fields, we plot the field in the plane $z = 0$.

Consider the field due to a 500-Hz spherical source at $(x, y, z) = (2.5, 0, 0)$. Figs. 5–7 show the results obtained using the mode-matching method without regularization. The pressure is shown in Fig. 5. (The pressure magnitude has been limited to a maximum of 0.5 to allow the wavefronts to be seen more easily.) The field is approximately correct up to a radius of 1 m and demonstrates interference effects outside this radius. The relative error shown in Fig. 6 has a peak of more than 5. (For clarity the error has been plotted out to 1.8 m to avoid larger peaks near individual loudspeakers.) The magnitudes of the weights plotted as a function of azimuth are shown in Fig. 7. These are maximum near the angle of incidence, but there are also relatively large values for loudspeakers far from this angle. The field plotted on the x axis is also shown in Fig. 7, which allows a closer comparison with the ideal field. The match is good for $|x| < 0.6$ m.

The equivalent results using the unwindowed simple source approach are shown in Figs. 8–10. The field in Fig. 8 has less interference than the mode-matching field, and the error in Fig. 9 is smaller than that in Fig. 6. The simple source weight magnitudes in Fig. 10 are smaller at angles away from the angle of incidence, which explains the reduced interference effects in the field of Fig. 8. The x-axis field is slightly smaller in error than in Fig. 7.

Figs. 11 and 12 show the mode-matching field for the same source position, but with a regularization parameter of $b = 2$. The field is less accurate near the origin, but the error is reduced at large radii, as expected. The loudspeaker weights are reduced at angles far from the angle of incidence, which reduces interference effects in the field.

Figs. 13 and 14 show the simple source result with a windowing function with exponential parameter of 0.5 and Kaiser parameter of 1.5. The field is more accurate than

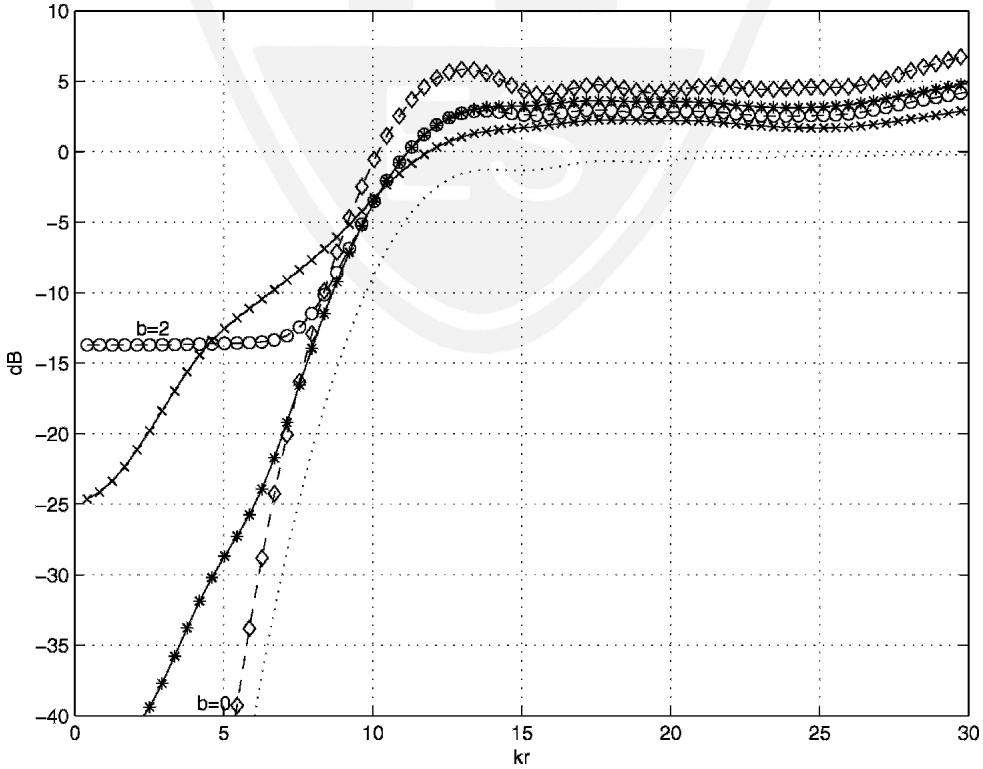

Fig. 4. Simple source (*), windowed simple source (×), mode-matching error (◇), and regularized mode-matching (○) error for 100-loudspeaker array at 2-m radius, source at 2.5 m. . . . Truncation error.

the regularized mode-matching field near the origin, and has a smoother and lower error than the regularized mode-matching form in Fig. 12. The weights in Fig. 14 are also reduced in relation to the peak at large azimuth angles, compared to Fig. 10.

Fig. 15 shows the field for a 4-kHz sperhical source at the same position. The field is accurate to about 0.1 m, which shows that a field in the region of a single listener can be produced using 100 loudspeakers, consistent with Table 1.

The field in the (x, z) plane is shown in Fig. 16 for a 4-kHz source at an elevation of 45° and a 5-m radius to demonstrate that wavefronts can be produced at orientations other than perpendicular to the (x, y) plane.

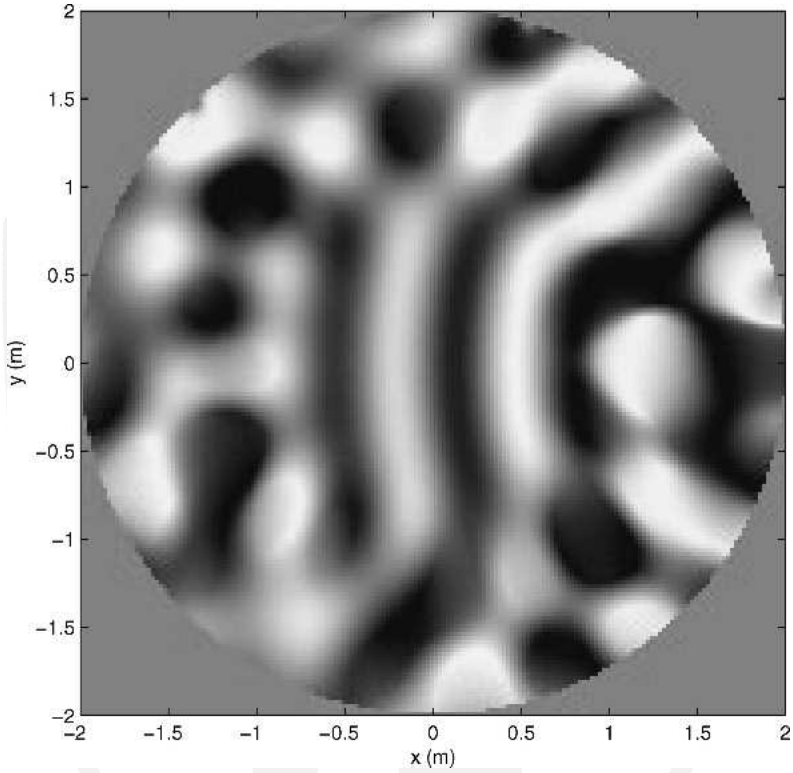

Fig. 5. Mode-matching field for 500-Hz source at 2.5 m, without regularization, using 100 loudspeakers.

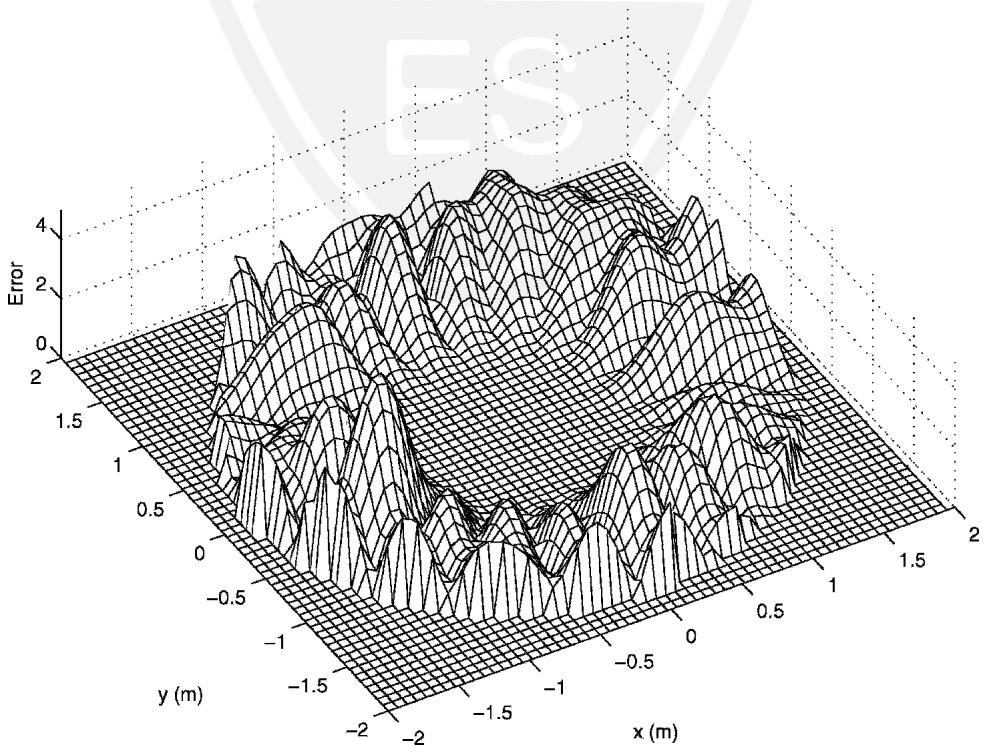

Fig. 6. Mode-matching error for 500-Hz source at 2.5 m without regularization, using 100 loudspeakers.

Finally it has been demonstrated in [9], [23], [24] that both WFS and Ambisonics can create point sound sources inside the loudspeaker array. The creation of source positions close to the origin is an ill-posed problem, producing small singular values in the mode matrix. This produces large loudspeaker amplitudes in the mode-matching solution. The simple source solution maintains lower amplitudes and less accuracy than the mode-matching solution.

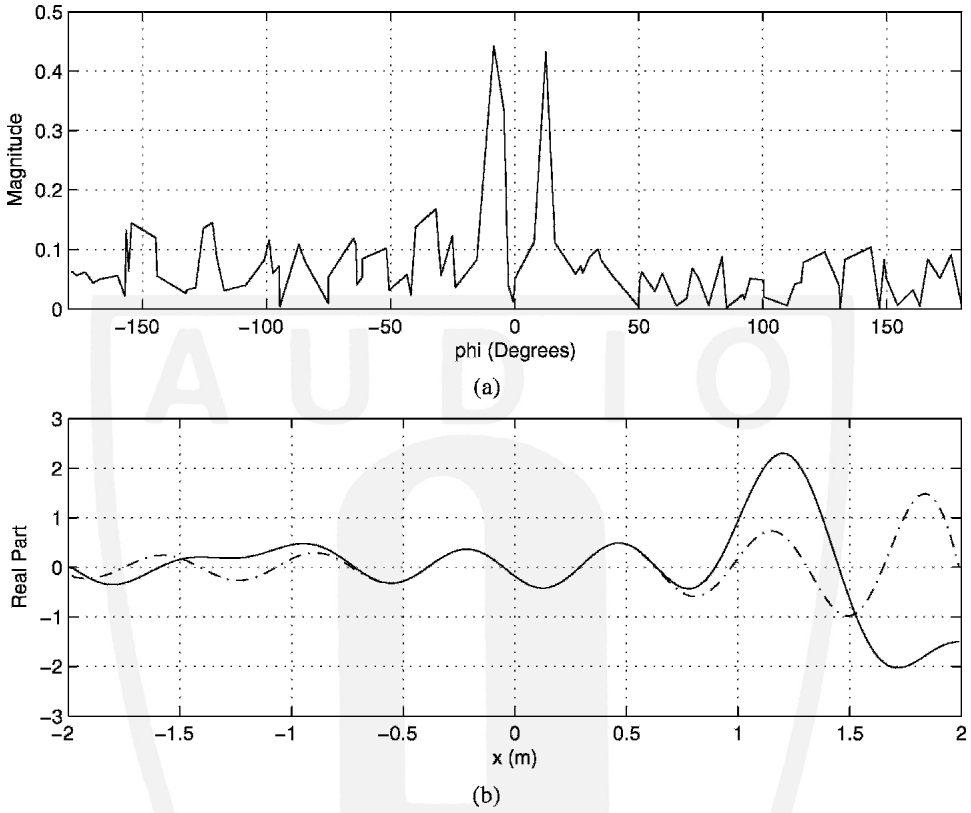

Fig. 7. (a) Mode-matching weights for 500-Hz source at 2.5 m without regularization, using 100 loudspeakers. (b) Field on x axis.

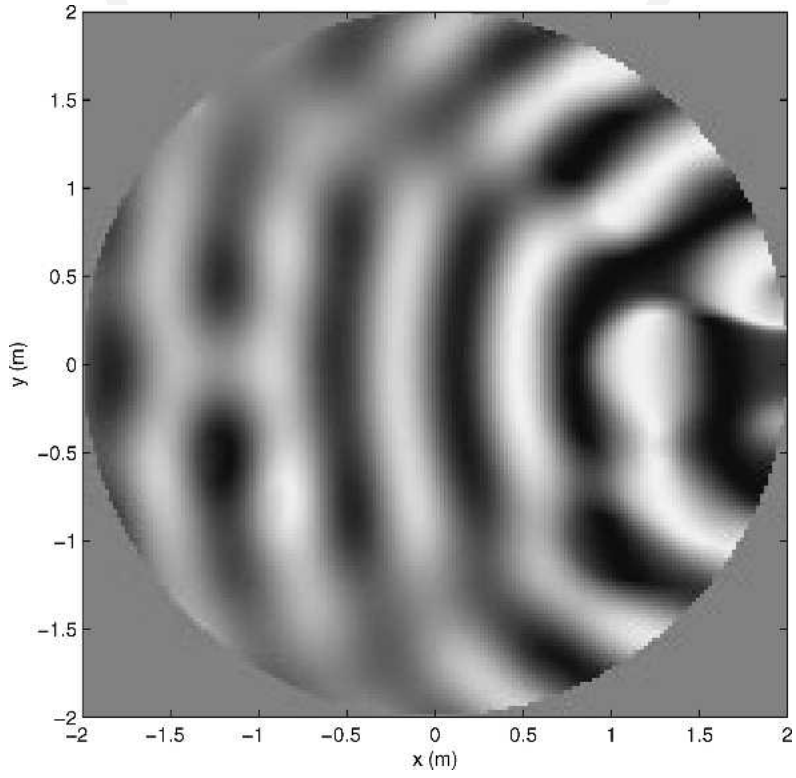

Fig. 8. Simple source field for 500-Hz source at 2.5 m without windowing, using 100 loudspeakers.

However, the large amplitudes produced by the mode-matching solution would be limited by power amplifiers and loudspeaker dissipations, and so larger regularization is required in practice. Fig. 17 shows the simple source field generated for a point source at a radius of 1.2 m, using a 256-loudspeaker arrray at a 2-m radius, which allows spherical harmonics up to order 15 (the same order used for the 2D results in [9]). The same window parameters were used as before. The mode-matching solution producing a similar response required a large regularization factor of $b = 300$.

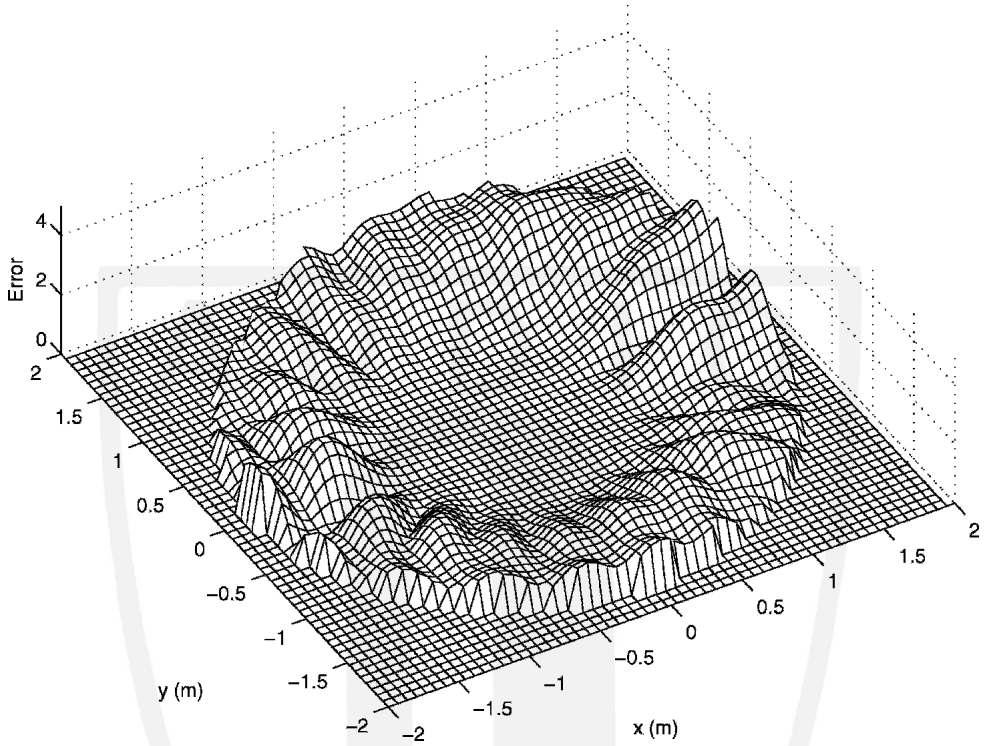

Fig. 9. Simple source error for 500-Hz source at 2.5 m without windowing, using 100 loudspeakers.

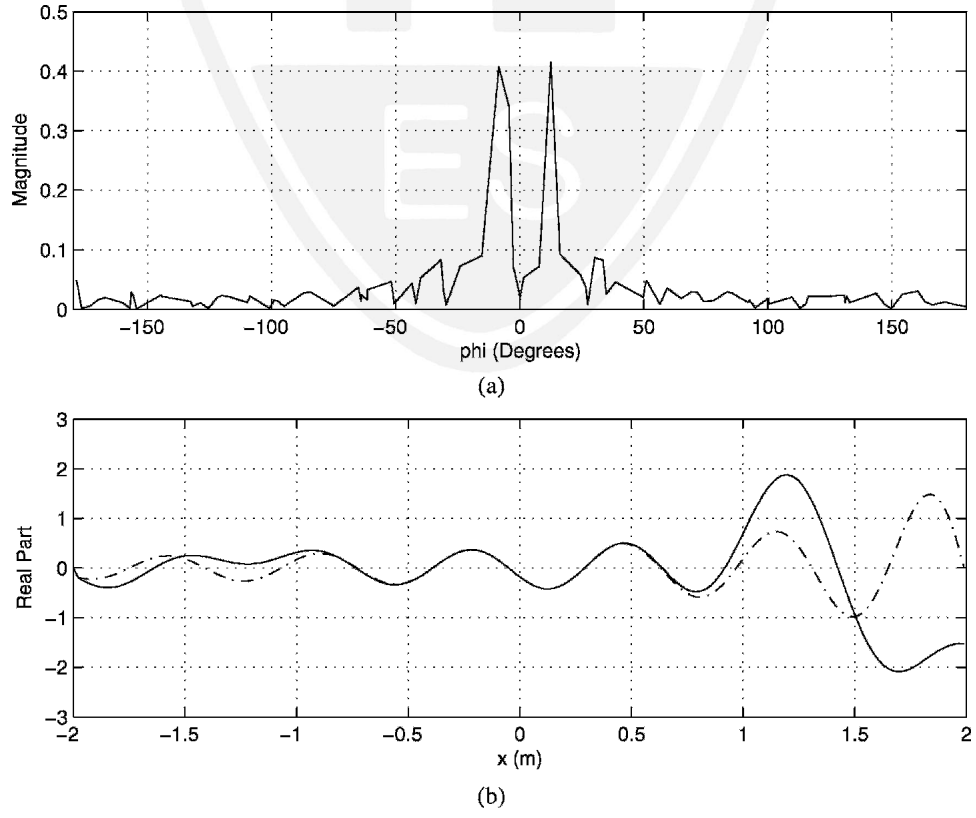

Fig. 10. (a) Simple source weights for 500-Hz source at 2.5 m without windowing, using 100 loudspeakers. (b) Field on x axis.

3.6 Extension to Reproduction in Reverberant Spaces

The mode-matching and simple source solutions derived in the preceding are applicable in free-field (anechoic) environments, or at least in rooms that are sufficiently damped so that reflections of the loudspeaker signals from the room surfaces do not affect the direct sound field generated by the loudspeakers significantly. For many listening rooms this requirement will not be met. Furthermore

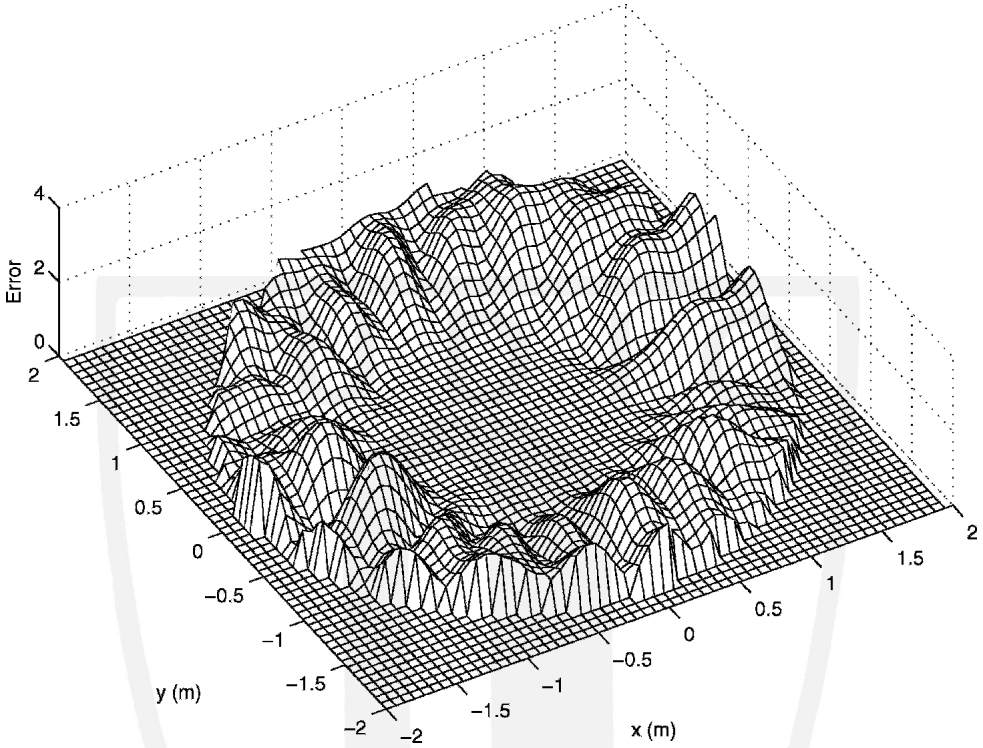

Fig. 11. Mode-matching error for 500-Hz source at 2.5 m with regularization parameter 2, using 100 loudspeakers (compare with Fig. 6).

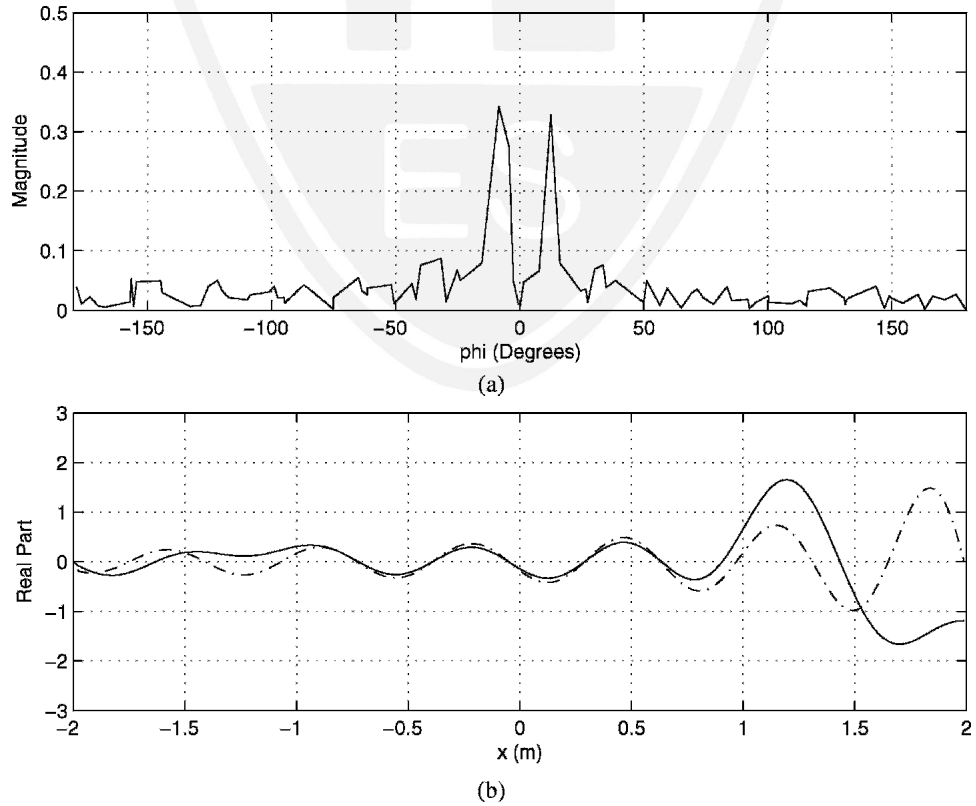

Fig. 12. (a) Mode-matching weights for 500-Hz source at 2.5 m with regularization parameter 2, using 100 loudspeakers. (b) Field on x axis (compare with Fig. 7).

the loudspeaker array may not be perfectly spherical, and the loudspeakers will not produce spherical waves at high frequencies. All of these conditions may be taken into account by extending the mode-matching solution to include the loudspeaker and room properties. This approach follows the 2D case discussed in [51].

Assume that there are L loudspeakers at arbitrary positions in a reverberant room. At each frequency at

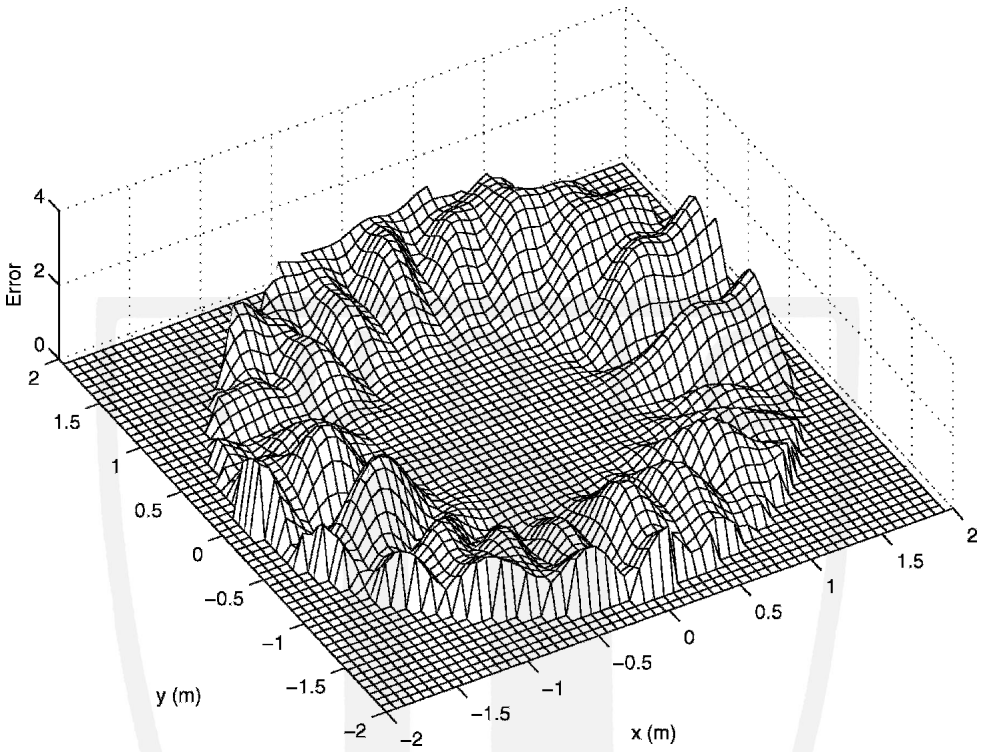

Fig. 13. Simple source error for 500-Hz source at 2.5 m with exponential window parameter 0.5 and Kaiser parameter 1.5.

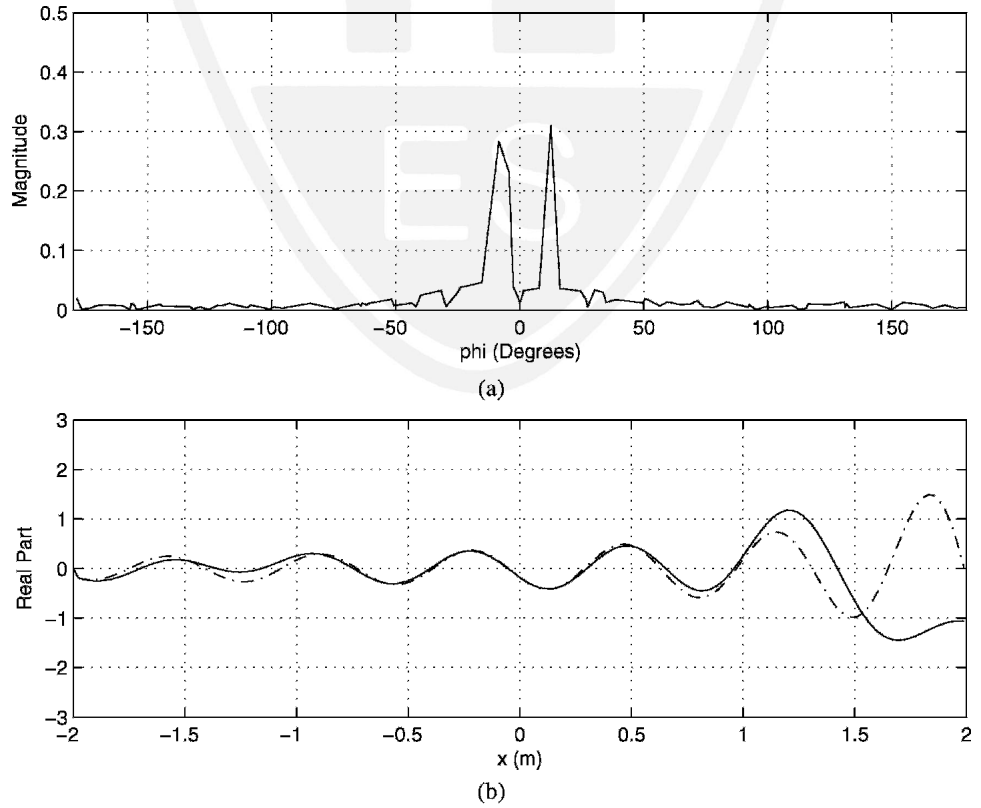

Fig. 14. (a) Simple source weights for 500-Hz source at 2.5 m with exponential window parameter 0.5 and Kaiser parameter 1.5, using 100 loudspeakers. (b) Field on x axis.

the listening position the *l*th loudspeaker produces a field in the region of the listening position (defined as the origin),

$$p_l(r, \theta, \phi, k) = \sum_{n=0}^{\infty} \sum_{m=-n}^{n} j_n(kr)\, Q_{n,l}^m(k)\, Y_n^m(\theta, \phi). \qquad (54)$$

The field coefficients $Q_{m,l}^m(k)$ may be measured by one of the methods described in Section 2.

To reproduce a desired sound field with measured coefficients $A_n^m(k)$ we apply a frequency-dependent amplitude weighting to each loudspeaker signal and require that the sum of the sound fields due to all L loudspeakers equal

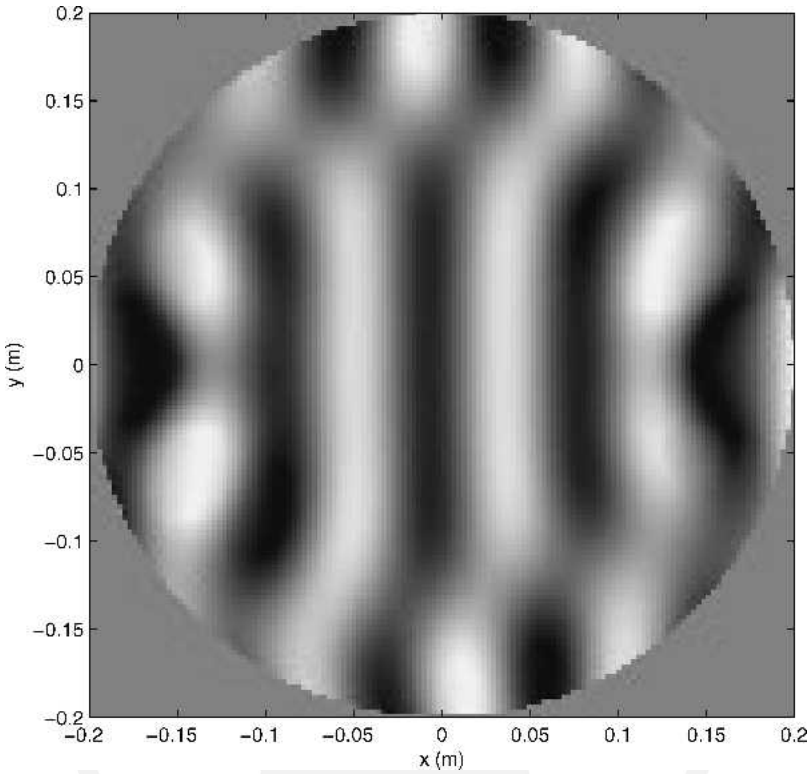

Fig. 15. Simple source field for 4-kHz source at 2.5 m without windowing.

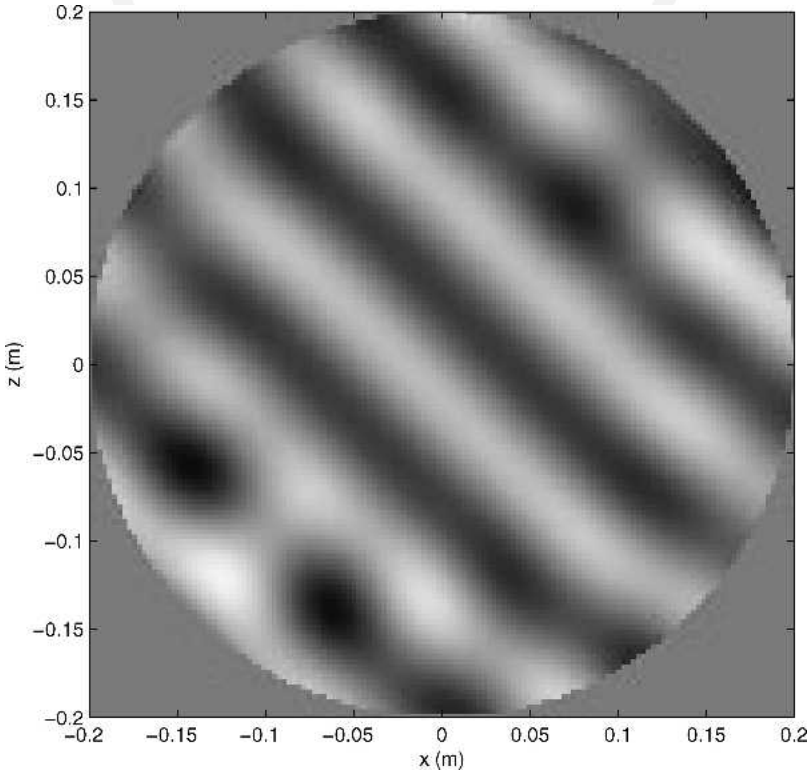

Fig. 16. Simple source field for 4-kHz source at 5 m, elevation 45°, azimuth 0°, without windowing.

the spherical harmonic decomposition of the desired field. This produces, for each term in the expansion,

$$\sum_{l=1}^{L} w_l(k)\, Q_{n,l}^m(k) = A_n^m(k). \tag{55}$$

Writing this equation for each l as a vector,

$$Q(k)\, w(k) = A(k) \tag{56}$$

where $Q(k)$ is an $(N+1)^2 \times L$ matrix with entries $Q_{n,l}^m(k)$. The loudspeaker weights may then be found as discussed in Section 3.2, depending on whether the number of loudspeakers L is less than or greater than the number of spherical harmonics. For example, for $L < (N+1)^2$ the regularized least-squares solution is

$$\hat{w}(k) = [Q^\dagger(k)\, Q(k) + \lambda I]^{-1}\, Q^\dagger(k)\, A(k) \tag{57}$$

where I is the $L \times L$ identity matrix. As an example we consider a spherical array of 100 ideal point source loudspeakers at a radius of 2 m (as in Section 3.5), in a rectangular room of dimensions 10 by 13 by 19 m. The sound field in the room is approximated by the spherical waves produced by every loudspeaker and N_m mirror sources [51], and so each entry of the mode matrix has the form

$$Q_{n,l}^m(k) = \mathrm{i}k \sum_{q=1}^{N_m} a_{q,l}\, h_n(kr_{q,l})\, Y_n^m(\theta_{q,l}, \phi_{q,l})^* \tag{58}$$

where the qth mirror source is at $(r_{q,l}, \theta_{q,l}, \phi_{q,l})$ and $a_{q,l}$ is the amplitude, derived from the wall absorption coefficient and distance. With a reverberation time of 0.5 s the wall absorption coefficient is 0.5, and using all mirror sources up to 8th order produced an impulse response with $N_m = 4913$ reflections and an impulse response length greater than 0.5 s, which is sufficient to approximate the reverberant field. The desired field is a single point source of radius 2.5 m along the x axis. The field produced using the mode-matched weights for the free-field case [Eq. (41)] is shown in Fig. 18 and the error in Fig. 19 (compare with Figs. 5 and 6). The ideal field is somewhat corrupted by the room reflections. This error would be larger in a smaller room where the mirror sources would be closer and produce larger pressures. Since the precedence effect may reduce the subjective effect of later reflections, the subjective significance of this interference as a function of room geometry and acoustics would require further study.

The field produced using Eq. (57) with no regularization ($\lambda = 0$) is shown in Fig. 20. The ideal field is now produced in the center of the array, and the field error is slightly greater than the free-field error in Fig. 5 at greater distances from the origin.

4 CONCLUSIONS

This paper has provided a review and further development of the continuous 3D theory of sound recording and reproduction based on the spherical harmonic expansion of the sound field. Spherical harmonics are well suited to describing sound reproduction over a localized volume of space and have application to other forms of localized sound reproduction such as virtual acoustics [54].

Three methods of recording 3D sound fields have been briefly reviewed. Spherical arrays of free-space directional

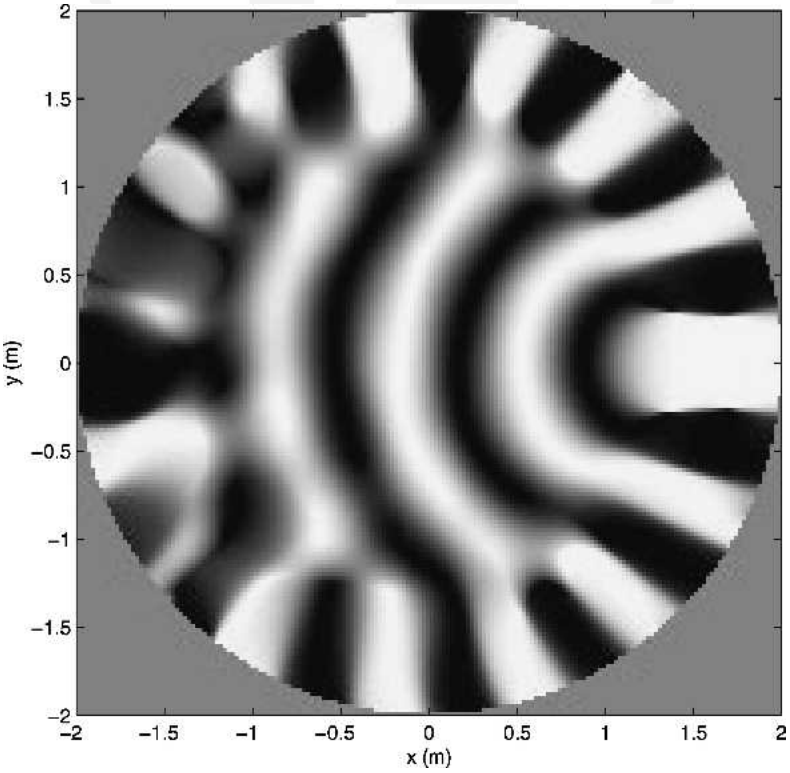

Fig. 17. Simple source field for point source at 1.2 m, on x axis, with exponential window parameter 0.5 and Kaiser parameter 1.5, using 256 loudspeakers.

microphones or sphere-mounted pressure microphones have been discussed. It has been shown that the free-field array mode responses are simpler to equalize than those of the solid sphere at low frequencies and that the sphere mode responses have a simplified form in terms of the derivative of a Hankel function. A general array method has also been discussed which allows the spherical harmonic coefficients to be determined using a pseudo inverse. A design issue for these arrays is the optimization of the microphone positions.

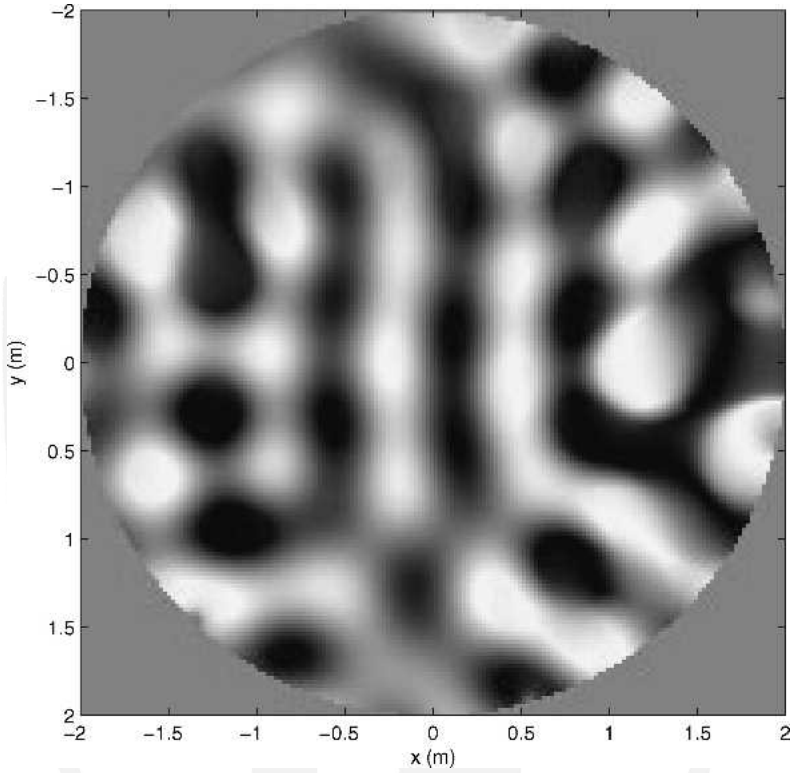

Fig. 18. Free-field mode-matching field for 500-Hz source at 2.5 m without regularization, using 100 loudspeakers at 2-m radius in a rectangular room of dimensions 10 by 13 by 19 m.

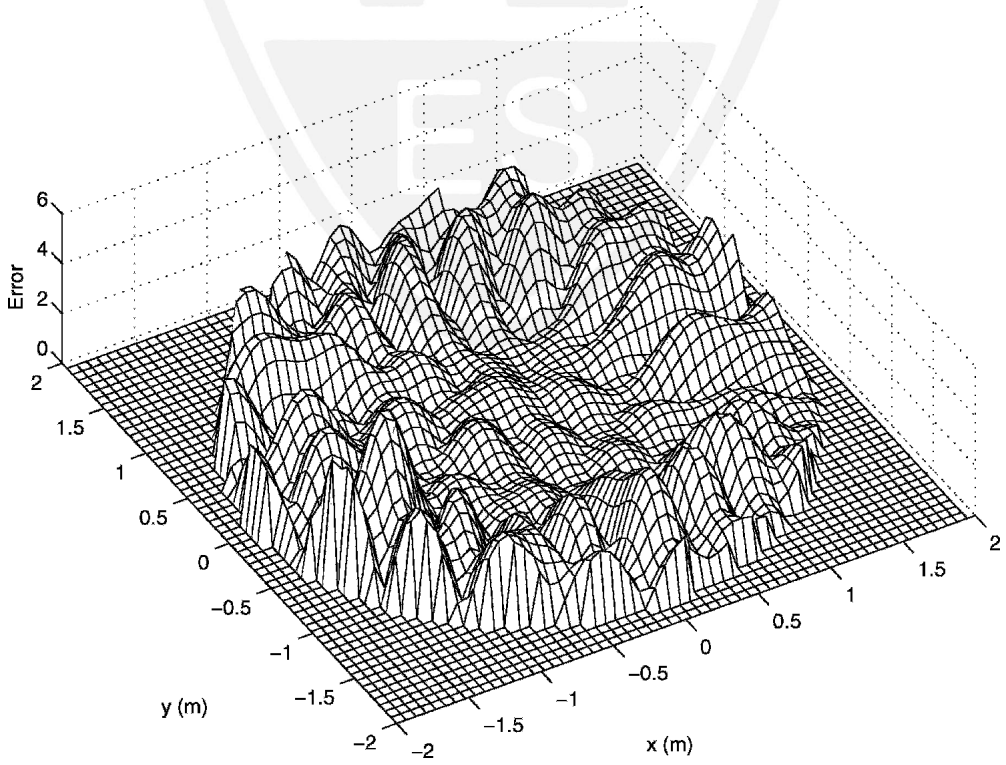

Fig. 19. Free-field mode-matching error for 500-Hz source at 2.5 m without regularization, using 100 loudspeakers, in a rectangular room of dimensions 10 by 13 by 19 m.

The sampling requirements for recording and reproducing 3D fields has been discussed briefly, and it has been shown that the number of transducers required for each process is similar.

Two approaches to sound reproduction in anechoic (or low-reverberance) environments have been presented. The mode-matching approach has been summarized, and the use of one form of regularization for controlling the loudspeaker amplitudes has been discussed. An alternative simple source approach has been derived which validates the use of the transpose of the mode matrix even if the loudspeaker array is not regular or if the mode matrix is nonunitary. The reconstruction error is lower than the mode-matching error wihout regularization, and windowing can be used to further control the error at high frequencies. Furthermore with appropriate windowing the error still tends to zero at the center of the array. The simple source approach also confirms that sound fields can be reconstructed without requiring dipole sources. It is possible that the regularized mode-matching approach can maintain accuracy at the origin using a different form of regularization, but this has not been investigated here.

It has also been shown that the mode-matching solution can be extended to the reproduction of sound fields in reverberant rooms and using more general loudspeaker arrays. The performance of the technique in a range of reverberant environments and its practical application remain future topics of research.

Key issues for 3D surround systems are the large data storage requirements and the complexity of the reproduction system. If calibration is required for reverberant spaces, then microphone arrays capable of measuring high-order spherical harmonics in the listening room are also required.

The storage requirements can be reduced by using a structured audio approach such as MPEG-4, in which sound sources are directly recorded and compressed and information on position and room environment is included [55]. Exact recording of the original sound field would not be required, but the reproduction system described here could be used to synthesize the required sound sources and room acoustics. Alternatively, the use of multichannel lossless coding [56], [57] and new high-capacity DVD recording media could allow the storage of a large number of channels to retain full recording and reproduction of holographic sound fields.

The reproduction system requires a number of loudspeakers, which rises quadratically with the reproduction frequency. The cost may be reduced by using a small number of woofers and a larger number of tweeters, and the tweeters could be flat panel transducers, which may be able to be incorporated into wall coverings.

5 ACKNOWLEDGMENT

The author would like to thank P. Teal for discussions during the course of this work.

6 REFERENCES

[1] M. A. Gerzon, "Ambisonics in Multichannel Broadcasting and Video," *J. Audio Eng. Soc.,* vol. 33, pp. 859–871 (1985 Nov.).

[2] J. S. Bamford, "An Analysis of Ambisonics Sound Systems of First and Second Order," *M.Sc. Thesis,* University of Waterloo, Waterloo, Ont., Canada (1995).

[3] J. S. Bamford and J. Vanderkooy, "Ambisonic

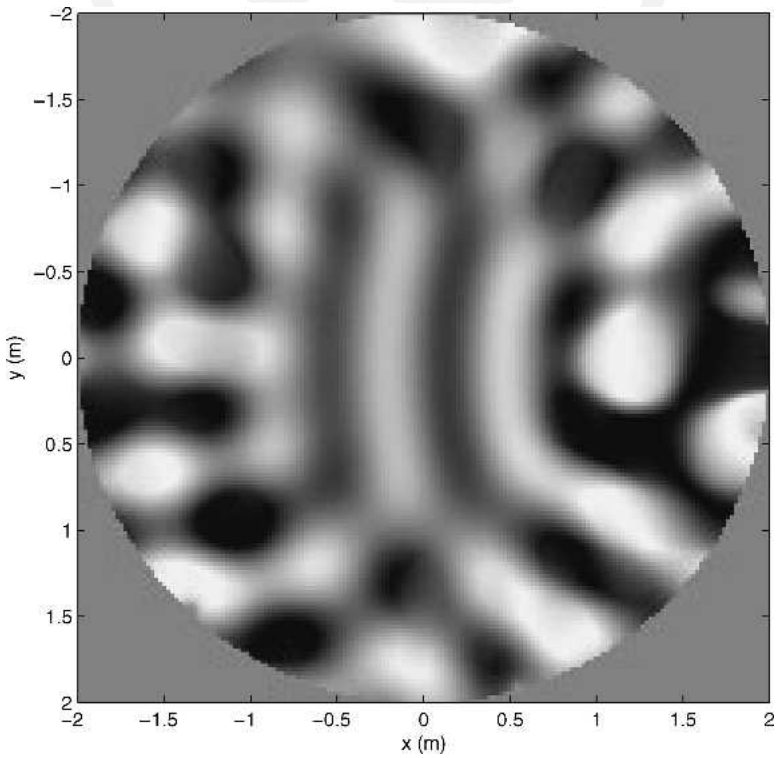

Fig. 20. Reverberant-field mode-matching error for 500-Hz source at 2.5 m without regularization, using 100 loudspeakers, in rectangular room of dimensions 10 by 13 by 19 m.

Sound for Us," presented at the 99th Convention of the Audio Engineering Society, *J. Audio Eng. Soc.* (*Abstracts*), vol. 43, p. 1095 (1995 Dec.), preprint 4138.

[4] D. H. Cooper and T. Shiga, "Discrete-Matrix Multichannel Stereo," *J. Audio Eng. Soc.,* vol. 20, pp. 346–360 (1972 June).

[5] M. A. Poletti, "The Design of Encoding Functions for Stereophonic and Polyphonic Sound Systems," *J. Audio Eng. Soc.,* vol. 44, pp. 948–963 (1996 Nov.).

[6] M. A. Poletti, "A Unified Theory of Horizontal Holographic Sound Systems," *J. Audio Eng. Soc.,* vol. 48, pp. 1155–1182 (2000 Dec.).

[7] M. Gerzon, "Periphony: With-Height Sound Reproduction," *J. Audio Eng. Soc.,* vol. 21, pp. 2–10 (1973 Jan/Feb.).

[8] D. G. Malham and A. Myatt, "3-D Sound Spatialization Using Ambisonics Techniques," *Computer Music J.,* vol. 19, no. 4, pp. 58–70 (1995).

[9] J. Daniel, R. Nicol, and S. Moureau, "Further Investigations of High-Order Ambisonics and Wavefield Synthesis for Holophonic Sound Imaging," presented at the 114th Convention of the Audio Engineering Society, *J. Audio Eng. Soc.* (*Abstracts*), vol. 51, p. 425 (2003 May), convention paper 5788.

[10] J. Daniel, "Spatial Sound Encoding Including Near Field Effect: Introducing Distance Coding Filters and a Viable New Ambisonics Format," presented at the AES 23rd International Conference, Copenhagen, Denmark (2003).

[11] J. Daniel, "Representation de Champs Acoustiques, Application à la Transmission et à la Reproduction de Scenes Sonores Complexes dans un Contexte Multimedia," Ph.D. Thesis, University of Paris 6, Paris, France (2000).

[12] R. Nicol and M. Emerit, "3D-Sound Reproduction over an Extensive Listening Area: A Hybrid Method Derived from Holophony and Ambisonic," presented at the AES 16th International Conference, Rovaniemi, Finland (1999).

[13] R. Nicol, "Restitution Sonore Spatialise sur une Zone Tendue: Application à la Tèlèprèsence," Ph.D. Thesis, Université du Maine (1999).

[14] A. Sontacchi and R. Holdrich, "Optimisation Criteria for Distance Coding in 3D Sound Fields," presented at the AES 24th International Conference, Banff, Canada (2003).

[15] J. Daniel, J.-B. Rault, and J.-D. Polack, "Ambisonics Encoding of Other Audio Formats for Multiple Listening Conditions," presented at the 105th Convention of the Audio Engineering Society, *J. Audio Eng. Soc.* (*Abstracts*), vol. 44, pp. 1034, 1035 (1998 Nov.), preprint 4795.

[16] P. G. Craven, "Continuous Surround Panning for 5-Speaker Reproduction," presented at the AES 24th International Conference, Banff, Canada (2003).

[17] E. G. Williams, *Fourier Acoustics* (Academic Press, London, 1999).

[18] M. Camras, "Approach to Recreating a Sound Field," *J. Acoust. Soc. Am.,* vol. 43, pp. 1425–1431 (1967).

[19] A. J. Berkhout, D. de Vries, and P. Vogel, "Acoustic Control by Wave Field Synthesis," *J. Acoust. Soc. Am.,* vol. 93, pp. 2764–2778 (1993).

[20] M. M. Boone, E. N. G. Verheijen, and P. F. van Tol, "Spatial Sound-Field Reproduction by Wave-Field Synthesis," *J. Audio Eng. Soc.,* vol. 43, pp. 1003–1012 (1995 Dec.).

[21] D. de Vries, "Sound Reinforcement by Wavefield Synthesis: Adaptation of the Synthesis Operator to the Loudspeaker Directivity Characteristics," *J. Audio Eng. Soc.,* vol. 44, pp. 1120–1131 (1996 Dec.).

[22] A. J. Berkhout, D. de Vries, and J. J. Sonke, "Array Technology for Acoustic Wave Field Synthesis in Enclosures," *J. Acoust. Soc. Am.,* vol. 102, pp. 2757–2770 (1997).

[23] E. Hulsebos, D. de Vries, and E. Bourdillat, "Improved Microphone Array Configurations for Auralization of Sound Fields by Wave-Field Synthesis," *J. Audio Eng. Soc.,* vol. 50, pp. 779–790 (2002 Oct.).

[24] D. de Vries and M. M. Boone, "Wave Field Synthesis and Analysis Using Array Technology," in *Proc. IEEE Workshop on Applications of Signal Processing to Audio and Acoustics* (1999), pp 15–18.

[25] S. Takane, Y. Suzuki, and T. Sone, "A New Method for Global Sound Field Reproduction Based on Kirchhoff's Integral Equation," *Acustica—Acta Acustica,* vol. 85, pp. 250–257 (1999).

[26] S. Ise, "A Principle of Sound Field Control Based on the Kirchhoff–Helmholtz Integral Equation and the Theory on Inverse Systems," *Acustica—Acta Acustica,* vol. 85, pp. 78–87 (1999).

[27] P. G. Flikkema, "An Algebraic Theory of 3D Sound Synthesis with Loudspeakers," presented at the AES 22nd International Conference, Espoo, Finland (2002).

[28] P. A. Nelson, F. Orduna-Bustamante, and H. Hamada, "Multichannel Signal Processing Techniques in the Reproduction of Sound," *J. Audio Eng. Soc.,* vol. 44, pp 973–989 (1996 Nov.).

[29] P. A. Nelson, H. Hamada, and S. J. Elliot, "Adaptive Inverse Filters for Stereophonic Sound Reproduction," *IEEE Trans. Signal Process.,* vol. 40, pp. 1621–1623 (1992).

[30] M. Miyosi and Y. Kaneda, "Inverse Filtering of Room Acoustics," *IEEE Trans. Acoust., Speech, Signal Process.,* vol. 36, pp. 145–152 (1988).

[31] A. Romano, "Three-Dimensional Image Reconstruction in Audio," *J. Audio Eng. Soc.,* vol. 35, pp. 749–759 (1987 Oct.).

[32] G. Dickins and R. Kennedy, "Towards Optimal Sound-Field Representation," presented at the 106th Convention of the Audio Engineering Society, *J. Audio Eng. Soc.* (*Abstracts*), vol. 47, p. 525 (1999 June), preprint 4925.

[33] B. A. Cray, V. M. Evora, and A. H. Nuttall, "Highly Directional Acoustic Receivers," *J. Acoust. Soc. Am.,* vol. 113, pp. 1526–1532 (2003).

[34] M. Abramowitz and I. A. Stegun, *Handbook of Mathematical Functions with Formulas, Graphs and Mathematical Tables* (National Bureau of Standards, Washington, DC, 1972).

[35] D. Colton and R. Kress, *Inverse Acoustic and Elec-*

tromagnetic Scattering Theory, Applied Mathematical Sciences, vol. 93, 2nd ed. (Springer, New York, 1998).

[36] F. Khalil, J. P. Jullien, and A. Gilloire, "Microphone Array for Sound Pickup in Teleconference Systems," *J. Audio Eng. Soc.,* vol. 42, pp. 691–700 (1994 Sept.)

[37] B. N. Gover, J. G. Ryan, and M. R. Stinson, "Microphone Array Measurement System for Analysis of Directional and Spatial Variations of Sound Fields," *J. Acoust. Soc. Am.,* vol. 112, pt. 1, pp. 1980–1991 (2002).

[38] M. W. Hoffman and K. M. Buckley, "Robust Time-Domain Processing of Broadband Microphone Array Data," *IEEE Trans. Speech Audio Process.,* vol. 3, pp. 193–203 (1995).

[39] J. Berg and F. Rumsey, "Validity of Selected Spatial Attributes in the Evaluation of 5-Channel Microphone Techniques," presented at the 112th Convention of the Audio Engineering Society, *J. Audio Eng. Soc. (Abstracts*), vol. 50, p. 522 (2002 June), convention paper 5593.

[40] J. Merimaa, "Applications of a 3-D Microphone Array," presented at the 112th Convention of the Audio Engineering Society, *J. Audio Eng. Soc.* (*Abstracts*), vol. 50, p. 496 (2002 June), convention paper 5501.

[41] A. Laborie, R. Bruno, and S. Montoya, "A New Comprehensive Approach of Surround Sound Recording," presented at the 114th Convention of the Audio Engineering Society, *J. Audio Eng. Soc.* (*Abstracts*), vol. 51, p. 405 (2003 May), convention paper 5717.

[42] G. Weinreich and E. B. Arnold, "Method of Measuring Acoustic Radiation Fields," *J. Acoust. Soc. Am.,* vol. 68, pp. 404–411 (1980).

[43] T. D. Abhayapala and D. B. Ward, "Theory and Design of High Order Sound Field Microphones Using Spherical Microphone Array," in *Proc. IEEE Int. Conf. on Acoustics, Speech, and Signal Processing,* vol. 2 (2002), pp. 1949–1952.

[44] J. Meyer and G. Elko, "A Highly Scalable Spherical Microphone Array Based on an Orthonormal Decomposition of the Sound Field," in *Proc. IEEE Int. Conf. on Acoustics, Speech, and Signal Processing,* vol. 2 (2002), pp. 1781–1784.

[45] J. Meyer, "Beamforming for a Circular Microphone Array Mounted on Spherically Shaped Objects," *J. Acoust. Soc. Am.,* vol. 109, pp. 185–193 (2001).

[46] J. Meyer and T. Agnello, "Spherical Microphone Array for Spatial Sound Recording," presented at the 155th Convention of the Audio Engineering Society, *J. Audio Eng. Soc.* (*Abstracts*), vol. 51, pp. 1253, 1254 (2003 Dec.), convention paper 5975.

[47] R. A. Kennedy, T. D. Abhayapala, and H. M. Jones, "Bounds on the Spatial Richness of Multipath," in *Proc. 3rd Australian Communications Theory Workshop* (AusCTW), (Canberra, Australia, 2002, Feb. 4–5), pp. 76–80.

[48] H. M. Jones, R. A. Kennedy, and T. D. Abhayapala, "On Dimensionality of Multipath Fields: Spatial Extent and Richness," in *Proc. IEEE Conf. on Acoustics, Speech, and Signal Processing* (*ICASSP*) (2002), vol. III, pp. 2837–2840.

[49] O. Kirkeby and P. A. Nelson, "Reproduction of Plane Wave Sound Fields," *J. Acoust. Soc. Am.,* vol. 94, pp. 2992–3000 (1993).

[50] D. B. Ward and T. D. Abhayapala, "Reproduction of a Plane-Wave Sound Field Using an Array of Loudspeakers," *IEEE Trans. Speech Audio Process.,* vol. 9, pp. 697–707 (2001).

[51] T. Betlehem and T. Abhayapala, "Theory and Design of Sound Field Reproduction in Reverberant Rooms," *J. Acoust. Soc. Am.,* vol. 117, pt. 1, pp. 2100–2111 (2005 April).

[52] C. P. Brown and R. O. Duda, "A Structural Model for Binaural Sound Synthesis," *IEEE Trans. Speech Audio Process.,* vol. 6, pp. 476–488 (1998).

[53] J. Fliege, "Integration Nodes for the Sphere," www.mathematik.unidortmund.de/lsx/research/projects/fliege/nodes/nodes.html.

[54] M. J. Evans, J. A. S. Angus, and A. I. Tew, "Analyzing Head-Related Transfer Function Measurements Using Surface Spherical Harmonics," *J. Acoust. Soc. Am.,* vol. 104, pp. 2400–2411 (1998).

[55] R. Väänänen and J. Huopaniemi, "Advanced AudioBIFS: Virtual Acoustic Modeling in MPEG-4 Scene Description," *IEEE Trans. Multimedia,* vol. 6, pp. 661–675 (2004 Oct.).

[56] T. Liebchen, "An Introduction to MPEG-4 Audio Lossless Coding," in *Proc. Int. Conf. Acoustics, Speech, and Signal Processing* (2004 May), vol. III, pp. 1012–1015.

[57] T. Leibchen, "Lossless Audio Coding Using Adaptive Multichannel Prediction," presented at the 113th Convention of the Audio Engineering Society, *J. Audio Eng. Soc.* (*Abstracts*), vol. 50, p. 965 (2002 Nov.), convention paper 5680.

APPENDIX 1
PROOF OF SIMPLE SOURCE FORMULA

It is shown in [17] that a sound field may be reconstructed using monopole sources as

$$p(r, \theta, \phi, k) = \int\int_S \mu(\boldsymbol{r}_s, k) \frac{e^{ik|\boldsymbol{r}-\boldsymbol{r}_s|}}{4\pi|\boldsymbol{r}-\boldsymbol{r}_s|} \, dS \tag{59}$$

and that the simple source distribution $\mu(\boldsymbol{r}_s)$ solution is given by

$$\mu(\boldsymbol{r}_s, k) = \frac{\delta p_o(\boldsymbol{r}, k)}{\delta n} - \frac{\delta p_i(\boldsymbol{r}, k)}{\delta n} \tag{60}$$

where $p_o(\boldsymbol{r})$ is the exterior field produced by a source distribution confined within the surface S, and $p_i(\boldsymbol{r})$ is the interior field produced by a source distribution outside the surface, with the condition that the two fields be equal on the surface.

Since $p_i(\boldsymbol{r})$ is an interior field it has the expansion

$$p_i(r, \theta, \phi, k) = \sum_{n=0}^{\infty} \sum_{m=-n}^{n} A_n^m(k) \, j_n(kr) \, Y_n^m(\theta, \phi,). \tag{61}$$

Similarly the exterior field has the expansion

$$p_o(r, \theta, \phi, k) = \sum_{n=0}^{\infty} \sum_{m=-n}^{n} B_n^m(k) \, h_n(kr) \, Y_n^m(\theta, \phi). \tag{62}$$

Assuming a spherical surface of radius R and equating the two expansions yields

$$B_n^m(k) = \frac{j_n(kR)}{h_n(kR)} A_n^m(k). \tag{63}$$

Taking the radial derivative of Eqs. (61) and (62) and substituting Eq. (63) yields from Eq. (60) (noting that the normal n faces inwards),

$$\mu(R, \theta_s, \phi_s, k) = -k \sum_{n=0}^{\infty} \sum_{m=-n}^{n} \frac{A_n^m(k)}{h_n(kR)} \left[j_n(kR)\, h_n'(kR) - j_n'(kR)\, h_n(kR) \right] Y_n^m(\theta_s, \phi_s). \tag{64}$$

The term in brackets is a Wronskian expression, which is equal to $\mathrm{i}/(kR)^2$. Hence,

$$\mu(R, \theta_s, \phi_s, k) = \sum_{n=0}^{\infty} \sum_{m=-n}^{n} \frac{A_n^m(k)}{\mathrm{i}kR^2 h_n(kR)} Y_n^m(\theta_s, \phi_s). \tag{65}$$

APPENDIX 2
CALCULATION OF RADIAL ERRORS FOR A SPHERICAL POINT SOURCE

A2.1 Average Squared Radial Pressure

The sound pressure due to a spherical source has the expansion in Eq. (10). The squared pressure required in Eq. (51) is

$$|p(r, \theta, \phi, k)|^2 = k^2 \sum_{n=0}^{\infty} \sum_{m=-n}^{n} \sum_{l=0}^{\infty} \sum_{q=-l}^{l} j_n(kr)\, j_l(kr)\, h_n(kr_s)\, h_l(kr_s) \times Y_n^m(\theta, \phi)\, Y_l^q(\theta, \phi)^*\, Y_n^m(\theta_s, \phi_s)^*\, Y_l^q(\theta, \phi). \tag{66}$$

Integrating over all angles, the orthogonality of the spherical harmonics produces

$$\int_0^{2\pi} \int_0^{\pi} |p(r, \theta, \phi, k)|^2 \sin(\theta)\, \mathrm{d}\theta\, \mathrm{d}\phi = k^2 \sum_{n=0}^{\infty} \sum_{m=-n}^{n} j_n^2(kr) \times |h_n(kr_s)|^2 |Y_n^m(\theta_s, \phi_s)|^2. \tag{67}$$

The summation in m is, from the addition theorem [35],

$$\sum_{m=-n}^{n} |Y_n^m(\theta,\phi)|^2 = \frac{2n+1}{4\pi} \tag{68}$$

and so the average squared pressure is

$$|p(r, k)|^2 = \int_0^{2\pi} \int_0^{\pi} |p(r, \theta, \phi, k)|^2 \sin(\theta)\, \mathrm{d}\theta\, \mathrm{d}\phi = \frac{k^2}{4\pi} \sum_{n=0}^{\infty} (2n+1)\, j_n^2(kr) |h_n(kr_s)|^2. \tag{69}$$

A2.2 Truncation Error

From Eq. (10) the truncation error for a spherical source is

$$\varepsilon_T(r, \theta, \phi, k) = p(r, \theta, \phi, k) - p_N(r, \theta, \phi, k) = \mathrm{i}k \sum_{n=N+1}^{\infty} j_n(kr)\, h_n(kr_s) \sum_{m=-n}^{n} Y_n^m(\theta, \phi)\, Y_n^m(\theta_s, \phi_s)^*. \tag{70}$$

Integrating the squared error and employing the orthogonality of the spherical harmonics and Eq. (68) yields

$$\varepsilon(r, k) = \frac{k^2}{4\pi} \sum_{n=N+1}^{\infty} (2n+1)\, j_n^2(kr) |h_n(kr_s)|^2 \tag{71}$$

which is of the same form as Eq. (69) but over the reduced summation range $N + 1$ to infinity. Hence the normalized squared truncation error is

$$\bar{\varepsilon}_T(r, k) = \frac{\sum_{n=N+1}^{\infty} (2n+1)\, j_n^2(kr) |h_n(kr_s)|^2}{\sum_{n=0}^{\infty} (2n+1) j_n^2(kr) |h_n(kr_s)|^2} = 1 - \frac{\sum_{n=0}^{N} (2n+1) j_n^2(kr) |h_n(kr_s)|^2}{\sum_{n=0}^{\infty} (2n+1) j_n^2(kr) |h_n(kr_s)|^2}. \tag{72}$$

A2.3 Reproduced Field Error

The error in the reproduced field is given by the difference between the field produced by the L loudspeakers with weights w and the ideal spherical source field,

$$\varepsilon_F(r, \theta, \phi, k) = \left[\sum_{l=1}^{L} w_l \frac{e^{\mathrm{i}k|\boldsymbol{r}-\boldsymbol{r}_l|}}{4\pi|\boldsymbol{r}-\boldsymbol{r}_l|} \right] - \frac{e^{\mathrm{i}k|\boldsymbol{r}-\boldsymbol{r}_s|}}{4\pi|\boldsymbol{r}-\boldsymbol{r}_s|}. \tag{73}$$

Substituting the spherical harmonic expansions of these two fields, the error can be expressed as

$$\varepsilon_F(r, \theta, \phi, k) = \mathrm{i}k \sum_{n=0}^{\infty} \sum_{m=-n}^{n} j_n(kr)\, Y_n^m(\theta, \phi) \left[h_n(kR) \sum_{l=1}^{L} w_l Y_n^m(\theta_l, \phi_l)^* - h_n(kr_s)\, Y_n^m(\theta_s, \phi_s)^* \right]. \tag{74}$$

The squared magnitude averaged over all angles is, following the same method as before,

$$\varepsilon_F(r, k) = k^2 \sum_{n=0}^{\infty} \sum_{m=-n}^{n} j_n^2(kr) |h_n(kR) \times \sum_{l=1}^{L} w_l Y_n^m(\theta_l, \phi_l)^* - h_n(kr_s)\, Y_n^m(\theta_s, \phi_s)|^2 \tag{75}$$

and so the normalized field error is

$$\bar{\varepsilon}_F(r, k) = 4\pi \left[\sum_{n=0}^{\infty} \sum_{m=-n}^{n} j_n^2(kr) |h_n(kR) \sum_{l=1}^{L} w_l Y_n^m(\theta_l, \phi_l)^* - h_n(kr_s)\, Y_n^m(\theta_s, \phi_s)^*|^2 \right] \times \left[\sum_{n=0}^{\infty} (2n+1) j_n^2(kr) |h_n(kr_s)|^2 \right]^{-1}. \tag{76}$$

The biography of M. A. Poletti was published in the 2005 May issue of the *Journal.*